Energy, Mines and Resources Canada | Energie, Mines et Ressources Canada

CANMET

Canada Centre for Mineral and Energy Technology | Centre canadien de la technologie des minéraux et de l'énergie

DESTRESSING A ROCKBURST PRONE CROWN PILLAR - MACASSA MINE

D. HANSON, W. QUESNEL AND R. HONG

ELLIOT LAKE LABORATORY

FEBRUARY 1987

MINING RESEARCH LABORATORIES
DIVISION REPORT MRL 87-82 (TR)

DESTRESSING A ROCKBURST PRONE CROWN PILLAR - MACASSA MINE

by

D. Hanson*, W. Quesnel** and R. Hong+

ABSTRACT

The use of destressing to avoid or control the timing of potential rockbursts has been a trial and error method for several years. In the Kirkland Lake mining camp destress blasting to control rock bursting has been attempted as early as the mid 1930's. High stress concentrations confined to brittle rock within crown pillars are increasing as mining below 1524 m is now the main ore producing area.

Macassa Division, Lac Minerals Ltd., designed a destress blast for the 58-40 crown pillar as previous rockburst activity and underground observations suggested that it was burst prone. In order to conduct a geotechnical appraisal of the destress blast, arrangements were made with CANMET to install a portable microseismic system and to assist in the interpretation of the seismic data.

The design and implementation of the destress blast involved evaluation of the characteristics of the destress application site, in situ instrumentation application, the requirements of an effective design, and cross-correlation with other methods such as computer mining simulation.

The effectiveness of the destress blast is discussed through a comparison of tape convergence results, microseismic source location activity, and a calibrated numerical model simulation of the destress blast. The results have an implication with respect to future mine extraction considerations when implementing destress blasting as a procedure at other locations in the mine.

Key words: Convergence; Microseismic activity; Destress blasting, Computer mining simulation.

*Ground Control Engineer, Elliot Lake Laboratory, CANMET, Energy, Mines and Resources Canada, Elliot Lake, Ontario.
**Rock Mechanics Engineer, +Rock Mechanics Technologist, Lac Minerals Ltd., Kirkland Lake, Ontario.

CONTENTS

TABLES

FIGURES

INTRODUCTION

The art of rock mass conditioning through destress blasting has had reasonable success in those circumstances where properly applied in order to initiate a timely rockburst, or to pre-condition the rock so that its strength is greatly reduced and avoid a rockburst. The depth of mining, per cent extraction, and material strength characteristics of the orebody versus the surrounding rock mass governs whether or not a remnant has the potential to fail violently or burst. Both depth of mining and extraction control the severity of stress loading on a remnant, but the potential for bursting is also controlled by the mine stiffness (hanging wall, footwall rockmass) in relation to the ore seam stiffness.

In the Macassa Mine where the steeply dipping ore vein consists of an interlayering of siliceous basic syenite, syenite porphyry and volcanic tuff, destress blasting has been successfully applied to crown pillars where visual observations and instrumentation have indicated high stress levels, seismic activity and ground deterioration. The preference is to situate the destress holes totally within the orebody and at the correct spacing to maintain a low powder factor. Only the intact pillar positions require direct exposure to explosives for destressing; hole sections in failed sections of a pillar are stemmed.

The determination of the success of a destress blast is dependent upon the before and after conditions evaluated through the underground instrumentation results (seismic activity location, tape convergence closure) and the assessment of ground deterioration. Another check is to compare the destressd area predicted using a computer mining simulation model with the destressed area from microseismic locations. As well, comparison of the computer model's predicted differential convergence after destressing should

be in agreement with the actual in situ differential convergence.

The purpose of this investigation was to examine a crown pillar where high stress conditions and rockbursts had designated it as burst prone. Follow up procedures involved evaluating site conditions through underground instrumentation, diamond drilling, visual observations, study of destress blast design layouts, incorporation of a localized MP-250 Electro-Lab microprocessor 'real time' source location system and geophone network, and comparison of the observed in situ conditions before and after the blast with those predicted by a 3-dimensional displacement discontinuity analysis method.

MINING AND GEOLOGICAL BACKGROUND

GENERAL GEOLOGY

The Macassa Division of Lac Minerals Ltd. is located 2.4 km west of the town of Kirkland Lake, Ontario. Over its 53 years of existence, Macassa has produced 76,543 kg of gold.

New reserves found in the western portion of the orebody, 2.4 km from existing shafts, resulted in the new No. 3 shaft being sunk from surface through the ore zone to a final depth of 2206 m.

The principal gold bearing veins of the Kirkland Lake camp occur along one of several fault systems called the Main Break. The main ore bearing structures located on the western extensions of this system are referred to as the '04' Break (Figure 1) and South Break. The structures are sub-parallel to the Main Break and the '04' Break has been the main ore source during the past thirty years.

The ore veinlets occur in quartz filled fractures which are closely associated with pre-ore faults and fractures and strike N 60^{o} E dipping 60-70^{o} to the South. Mining widths are commonly 2.5 m.

The geological events in the Kirkland Lake camp consisted of folding of

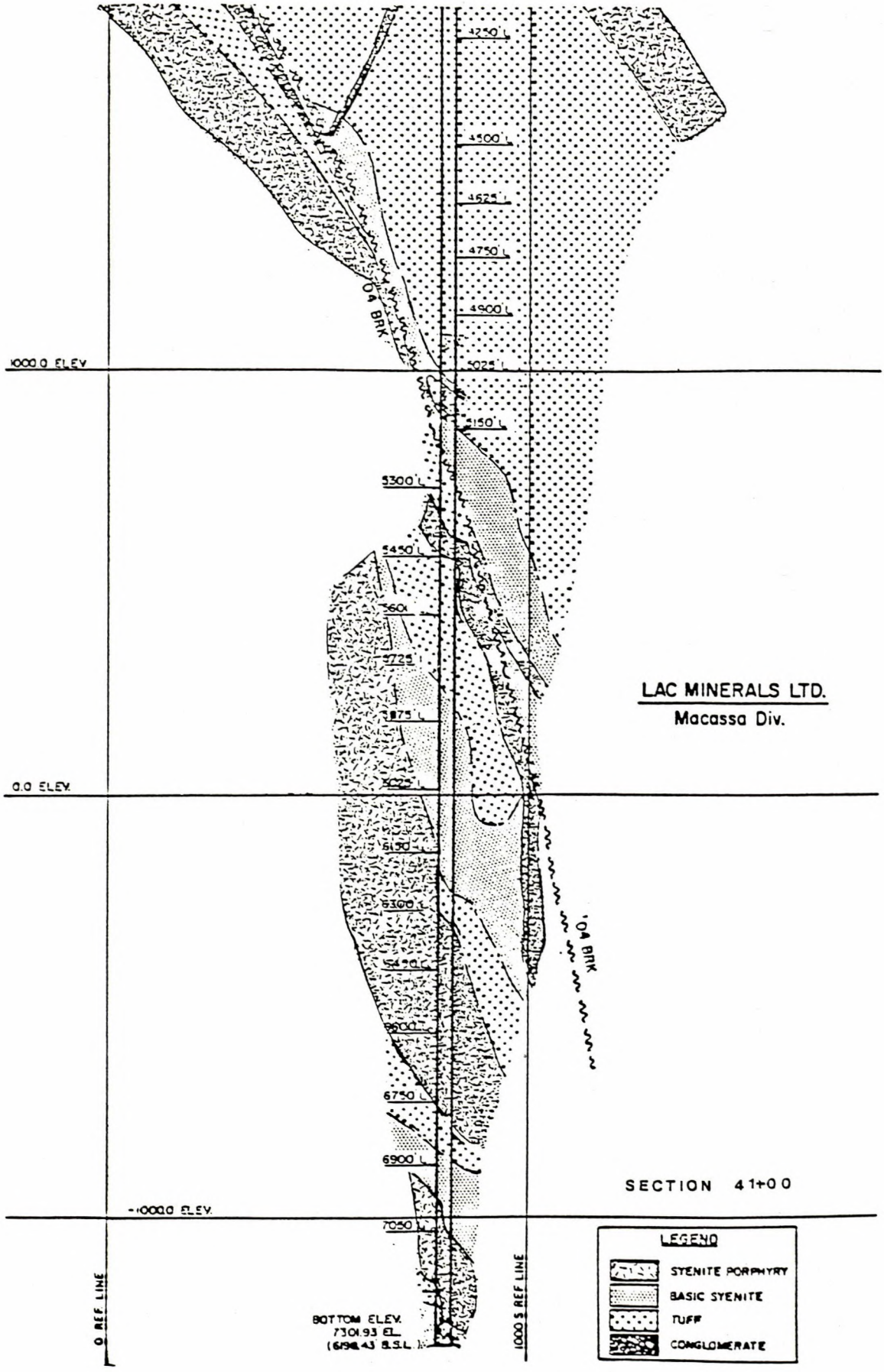

Fig. 1 - Geological section of No. 3 shaft area, Macassa Mine.

original sediments, intrusions of basic or felsic syenite, intrusion of the syenite porphyry, faulting (fracturing), gold deposition and remobilization along the faults, and post-ore faulting.

MINING METHODS

The major mining method at Macassa is overhand cut-and-fill with waste fill provided from a long hole waste stope and recycled mine development waste from mine headings.

Drilling with stopers and jacklegs is common with the fragmented ore drawn by slushers. A transition of mining method (to longwall blasting) commonly occurs at a crown pillar height of 15 m (Figure 2) as stress levels are substantial enough to promote rockbursts. Mining of the bottom half consists of steeply inclined blasted 'uppers' closely followed by horizontally blasted longholes (upper half) with the fragmented ore removed by slushers. The waste fill is kept in close proximity to the brow. Approximate stope dimensions are 60 m along strike, 45 m high and 2.5 m wide.

GEOTECHNICAL BACKGROUND

Laboratory testing results combined with in situ seismic velocity profiles are shown in Tables 1 and 2 for the various rock types.

Underground experience as well as evidence from Tables 1 and 2, shows that the tuff appears more prone to bursting than the other rocks, that the tuff and porphyry are more brittle than the basic syenite, and that the probability of bursting increases with increasing silica content. Areas where basic syenite constitutes the wall rock and tuff and/or porphyry the orebody could be more burst prone than others under high stress conditions.

In situ stress determinations completed by CANMET on two levels (5300 and 6300) near No. 3 shaft suggested the following stress with depth relationship:

$$V, \text{Vertical Stress} = 0.026 \text{ MPa/m (depth)}$$

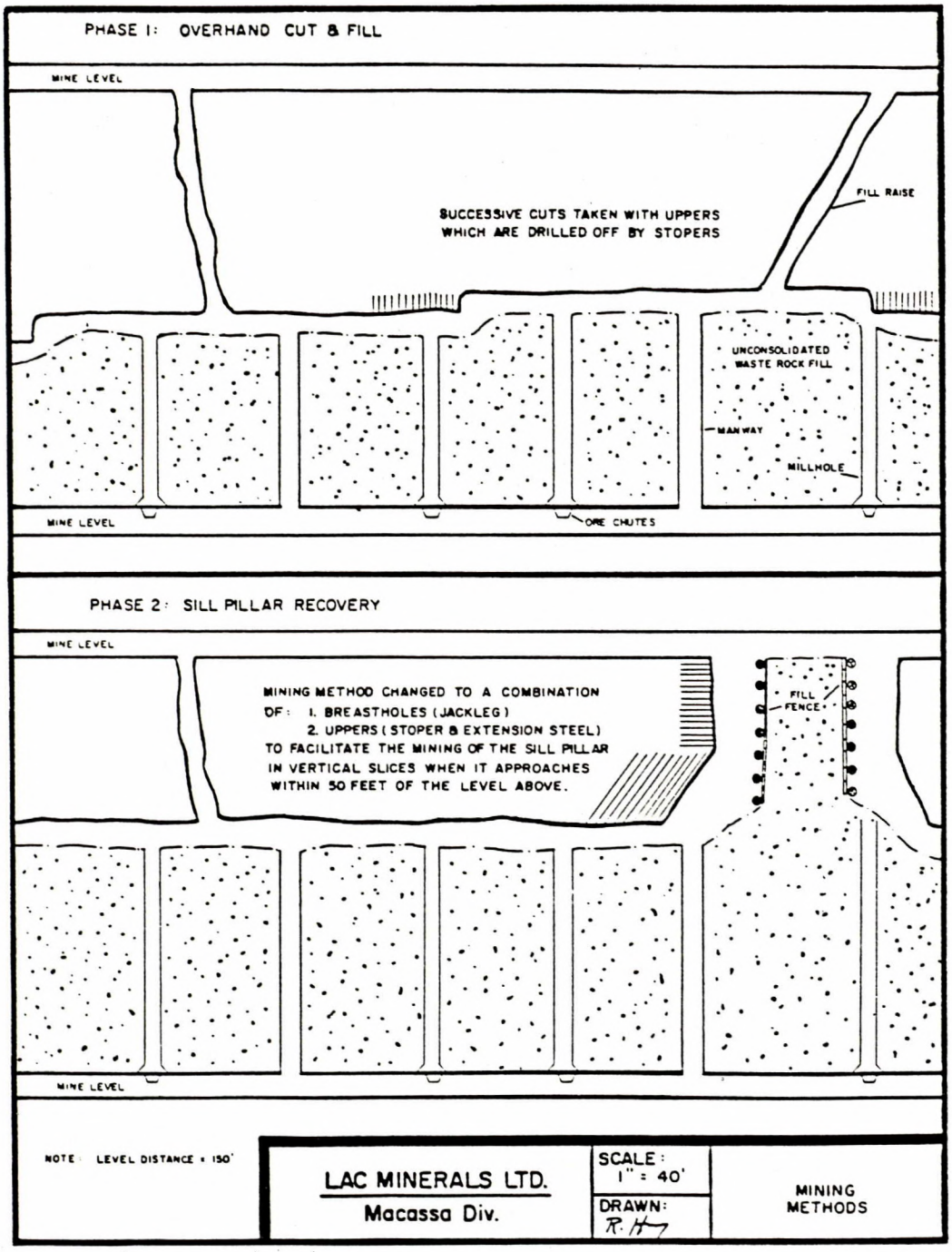

Fig. 2 - Mining transition phases for crown pillar recovery.

Table 1 - Laboratory rock property data.

Rock Type	Compressive Strength (MPa) Uniaxial	Triaxial (σ_3=13.8)	Mean Uniaxial Compressive Strength (MPa)	Modulus ($x10^3$) (MPa)	Poisson's Ratio	Theor. Stored Strain Energy (J/m^3)
Tuff	117-344	386	193	69	0.24	77-693
Porphyry	137-358	386	227	80	0.21	100-654
Basic syenite	110-193	317	144	80	0.20	57-192

Table 2 - In situ seismic data.

Rock Type	Mean Seismic Velocity (m/sec)	Calculated Elastic Properties (MPa) Elastic Modulus ($x10^3$)	Bulk Modulus ($x10^3$)
Tuff	5,638	70	28
Porphyry	6,096	96	29
Basic syenite	3,596	32	13
Basic sysenite c/w quartz stringers	4,663	54	22

Horizontal stress (Perpendicular to strike) = 1.62 V

Horizontal stress (Parallel to Strike) = 1.14 V

In the area of concern, premining stresses would be in the order of 70 MPa. Mining induced stresses result in an additional stress of 68.9 MPa based on the results of N-FOLD displacement discontinuity computer modelling studies completed earlier by Golder Associates, Mississauga, Ontario.

ROCKBURST HISTORY

As previously mentioned, the larger energy bursts at Macassa generally occur during mining of the crown pillars (Figure 3) at a critical geometry (height <15 m). Smaller strain bursts do occur in development headings but can be controlled by localized destressing procedures where destress holes are situated within the plane of the heading parallel to its long axis.

Where a crown pillar contains a stiff rock unit (tuff) in comparison to the wall rocks (i.e., basic syenite) and where stress levels are approaching the failure point, it is not uncommon to have a burst occur immediately after a production blast. Prior to a production blast several areas may be at critical stress levels (near failure). The act of mining may cause an incremental stress increase sufficient to generate violent failure and post-failure conditions at these same locations.

To reduce the risk of exposure to an untimely rockburst, various trial and error blast destressing schemes have been developed with a certain amount of variance with regard to hole spacing, powder factor, stemming, initiation, and explosive type.

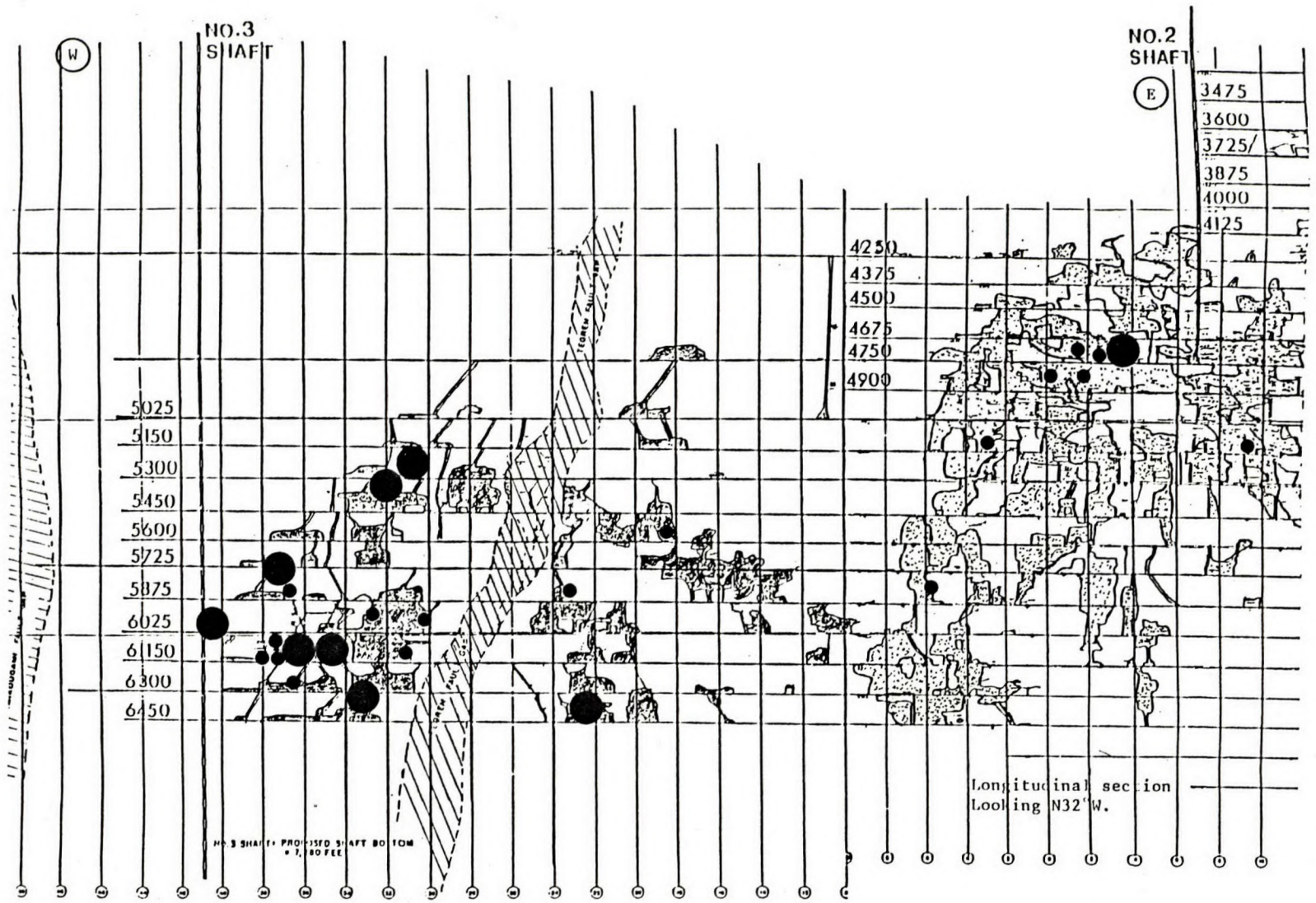

Fig. 3 - Location of rockbursts on the west and central area at the Macassa Mine. (●) Recorded rockbursts, magnitude 2.2 to 3.1 MN. (●) observed "heavy rockbursts", rock displacement >50 tons.

CHARACTERISTICS OF THE DESTRESS APPLICATION SITE

GEOLOGY

The geology within the 58-40 stope (Figure 4) consists of an interlayering of basic syenite, syenite porphyry and tuff. The eastern portion of the stope consists of silicified basic syenite seam material with basic syenite or porphyry in the hanging wall and basic syenite in the footwall. Towards the western area of the 58-40 stope the seam material consists of volcanic tuff within the ore zone as well as the footwall but basic syenite is dominant in the hanging wall.

The '04' Break forms the hanging wall of the stope in the western section of 58-40 but then cuts across the ore seam to form the footwall near the eastern 58-38 access raise. The break dips at 70-75^{o} and has a chlorite infilling only a few inches thick. Parallel to the '04' Break is another chlorite coated fault 1-2 m further into the hanging wall.

With the assemblage of rock types it appears that the silicified basic syenite and tuff which form a major portion of the seam material are of a higher modulus than that of the basic syenite wall material. The significance of this is that the stored strain energy within the seam material under high stress loading would appear to be greater than if the seam consisted of basic syenite (i.e., the same material properties as the rock wall).

Salamon (6) has shown that the act of mining (or rockbursts) results in the following:

$$(W_t + U_m) - (U_c + W_s) = W_r > 0 \qquad \text{Eq 1}$$

1) a change in the potential energy of the wall rocks, W_t
2) a release of stored strain energy in the mined seam, U_m
3) an increased strain energy transfer to the wall rocks, U_c
4) a small fraction of released potential energy stored in the backfill

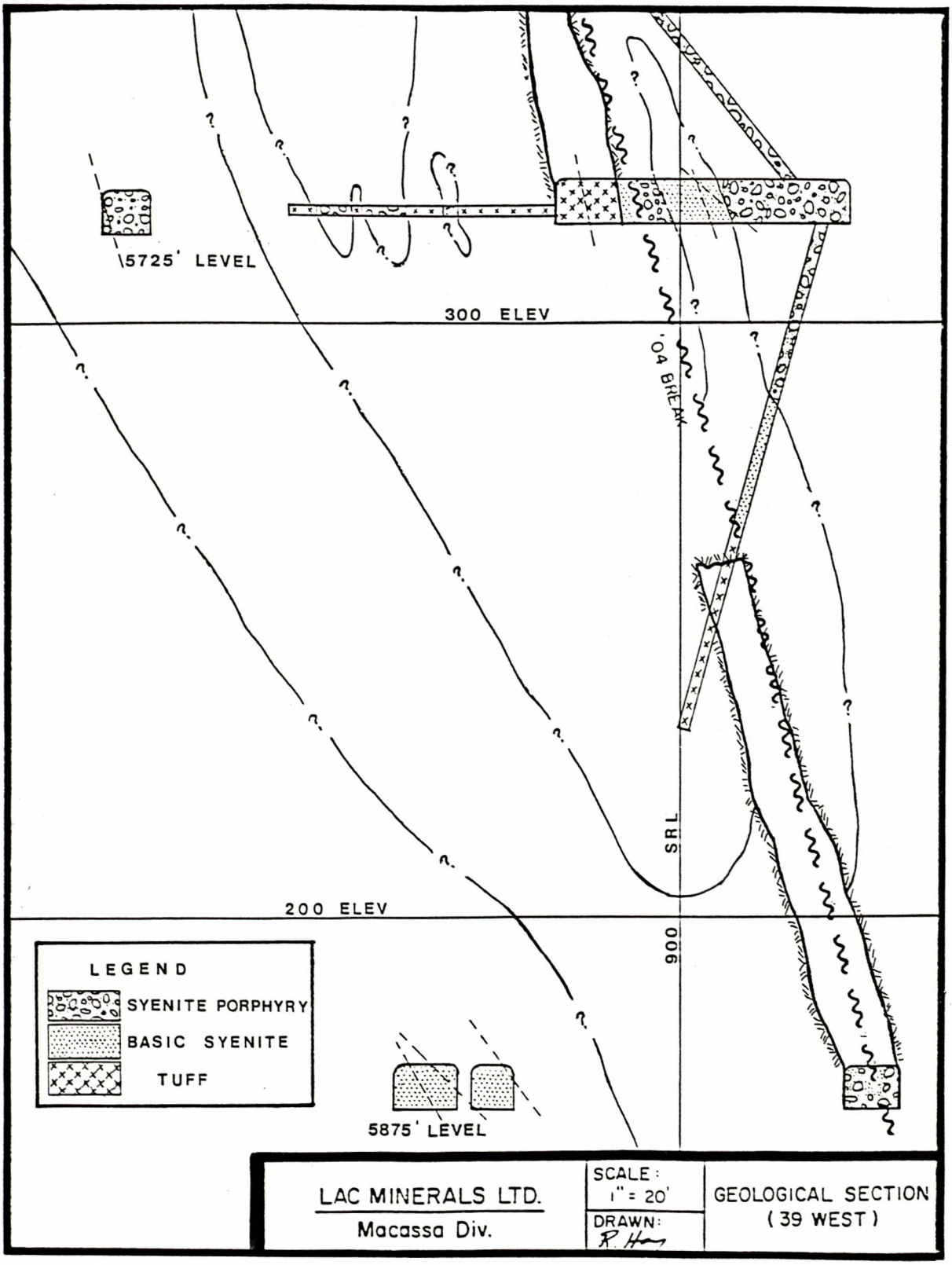

Fig. 4 - Rock type assemblage near the 58-40 cut-and-fill stope.

material, W_s

5) excess energy, W_r, (composed of kinetic energy, W_k + released stored strain energy, U_m)

Salamon has also shown that the condition for violent failure can be put into a mathematical inequality as follows:

$$K + \lambda \leq 0 \qquad \text{Eq 2}$$

where, K represents the hanging wall/footwall rock mass mine stiffness, and

λ represents the seam stiffness.

As mining takes place mine and seam (pillars) stiffnesses in the immediate area change. As critical pillar strength is approached λ approaches zero (horizontal slope). Upon failure it assumes a negative slope whose value is dependent on the pillar's brittleness and width to height ratio. Salamon's inequality suggests that when the mine stiffness (positive in nature) is exceeded by the post-failure λ (a negative quantity), critical instability can result.

The interrelation of the above factors suggests a greater release of energy in the form of a rockburst (kinetic energy and energy absorbed in mass fracturing) occurs when the stiffness of the seam material dominates over the mine stiffness. However, the greatest source of energy is the potential energy, W_t, created from the convergence of the wall rocks over a defined area. The stored strain energy is always a fraction of W_t.

MINING LAYOUT

The 58-40 stope was mined conventionally (55%) by cut-and-fill with the fill consisting of mined development waste. At a certain distance, 24.4 m above the 5875 level, deteriorating ground conditions and increased seismic activity suggested that the crown pillar had burst potential.

Remedial action involved considering the consequences of destress blasting and the transition over to a safer method of extraction.

ROCKBURST OCCURRENCE WITHIN THE 58-40 STOPE

Three separate documented rockbursts occurred within the 58-40 stope between July 1985 and January 1986 (Figure 5).

The first two rockbursts occurred shortly after stope production blasts; the third incident, a minor burst, was not triggered by blasting. The pertinent information is as follows:

Event	Date	Tons Displaced	Stope Location	Event Size	M_N
1	July 85	80	58-40 Raise	Major	-
2	Sept. 24,85	45	58-38 Raise	Major	2.4
3	Jan. 10,86	20	Stope Back	Intermediate	-

Production slowdowns resulted due to general clean-up and restoration of the workings as a result of the bursts. As the working environment was considered to be getting more hazardous it was felt destressing of the pillar at an early stage would be advisable. Drilling of the destress holes could be attempted in fairly competent rock.

INSTRUMENTATION

STRESS AND CONVERGENCE

An early objective of the rock mechanics group of Macassa Division, Lac Minerals, was to install stress and displacement monitoring devices in the near vicinity of the 58-40 crown pillar. The behavioural background if readings were taken for a long enough period would establish trends and provide early warning to changed site conditions.

Three diamond drill holes were drilled through the crown pillar at various locations so that vibrating wire (IRAD) strain gauges could be

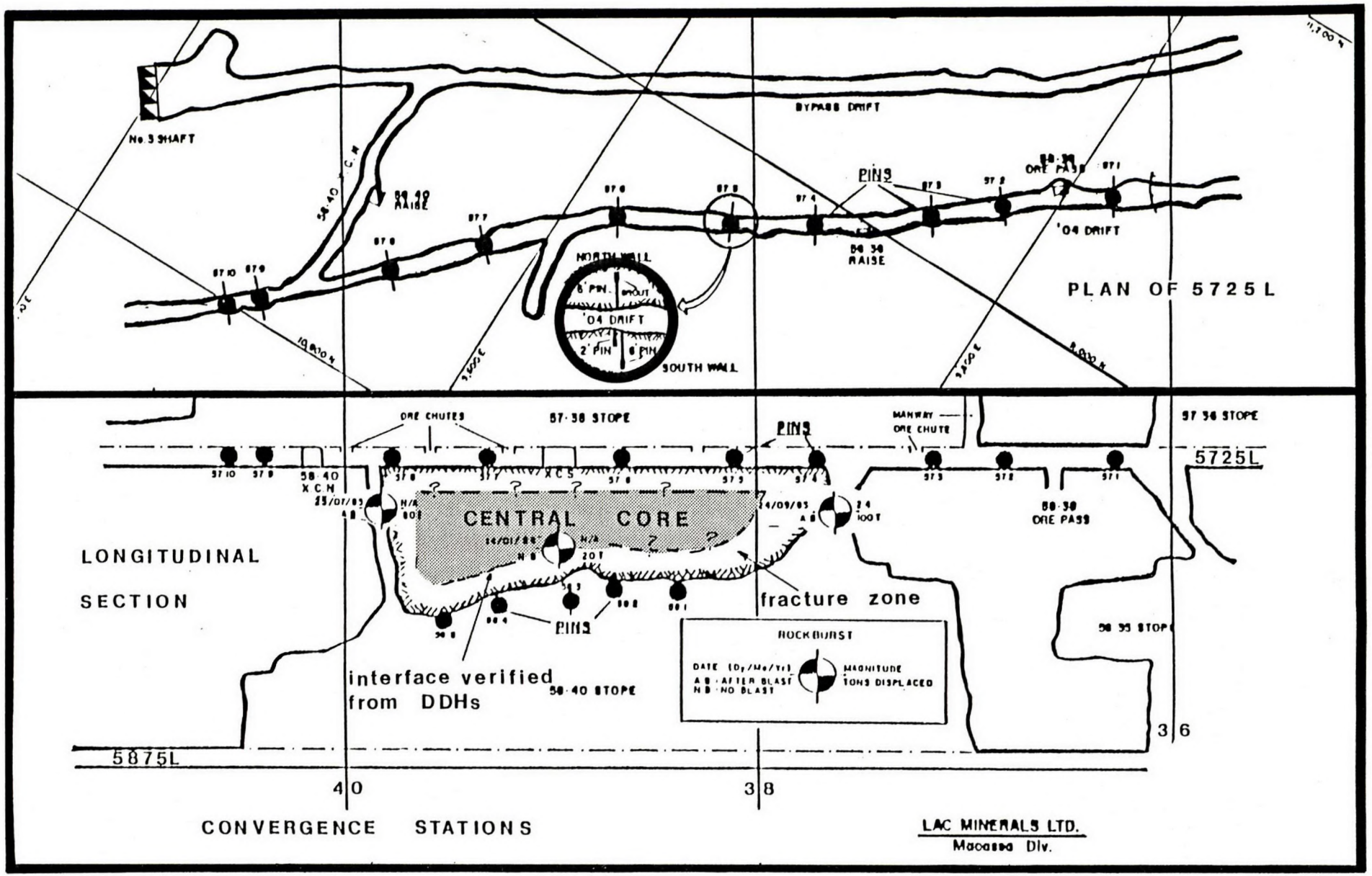

Fig. 5 - Convergence stations, rockburst activity, 58-40 crown pillar conditions.

installed to measure stress changes. The core was recovered from these holes, but a short time later a local rockburst collapsed the holes preventing strain gauge installation.

The diamond drill core did suggest, however, that a 'central core' of the pillar was 9-14 m wide with a peripheral 3 to 3.5 m fracture zone engulfing it (Figure 5).

Tape convergence points were established both along the 5725 level bordering the top edge of the 58-40 crown pillar and within the uppermost cut bordering the bottom outline of the pillar. Two sets of pins, one established on the hanging wall side of the strike drift, and one located on the hanging wall side of the chlorite coated hanging wall slip were installed on the 5725 level (Figure 5).

No attempt was made to redrill the IRAD gauge holes as it was felt this would delay initializing the drilling program for the destress holes.

MICROSEISMIC DATA ACQUISITION SYSTEM

Arrangements were made between CANMET (Elliot Lake Laboratory) and Lac Minerals to temporarily install a microseismic monitoring system with the microprocessor (Electro-Lab MP-250) located at the electrical sub-station on 5725 level and accelerometers in a tight array around the 58-40 crown pillar.

This system (Figure 6) consisted of an array of 12 Model 271 accelerometers (Electro-Lab) and a three axis energy phone for energy integration, with the analog signal carried to the Electro-Lab MP-250 microprocessor via shielded multiwire cable. Processing of the analog data to digital form provided real time data acquisition and display. A microseismic event of sufficient magnitude exceeding the preset threshold of 5 channels (the threshold set on background, process, or adjust) at the microprocessor resulted in a source location, energy level, time in hr:min:sec, Julian day, geophone identification and arrival times being sent to the standard output

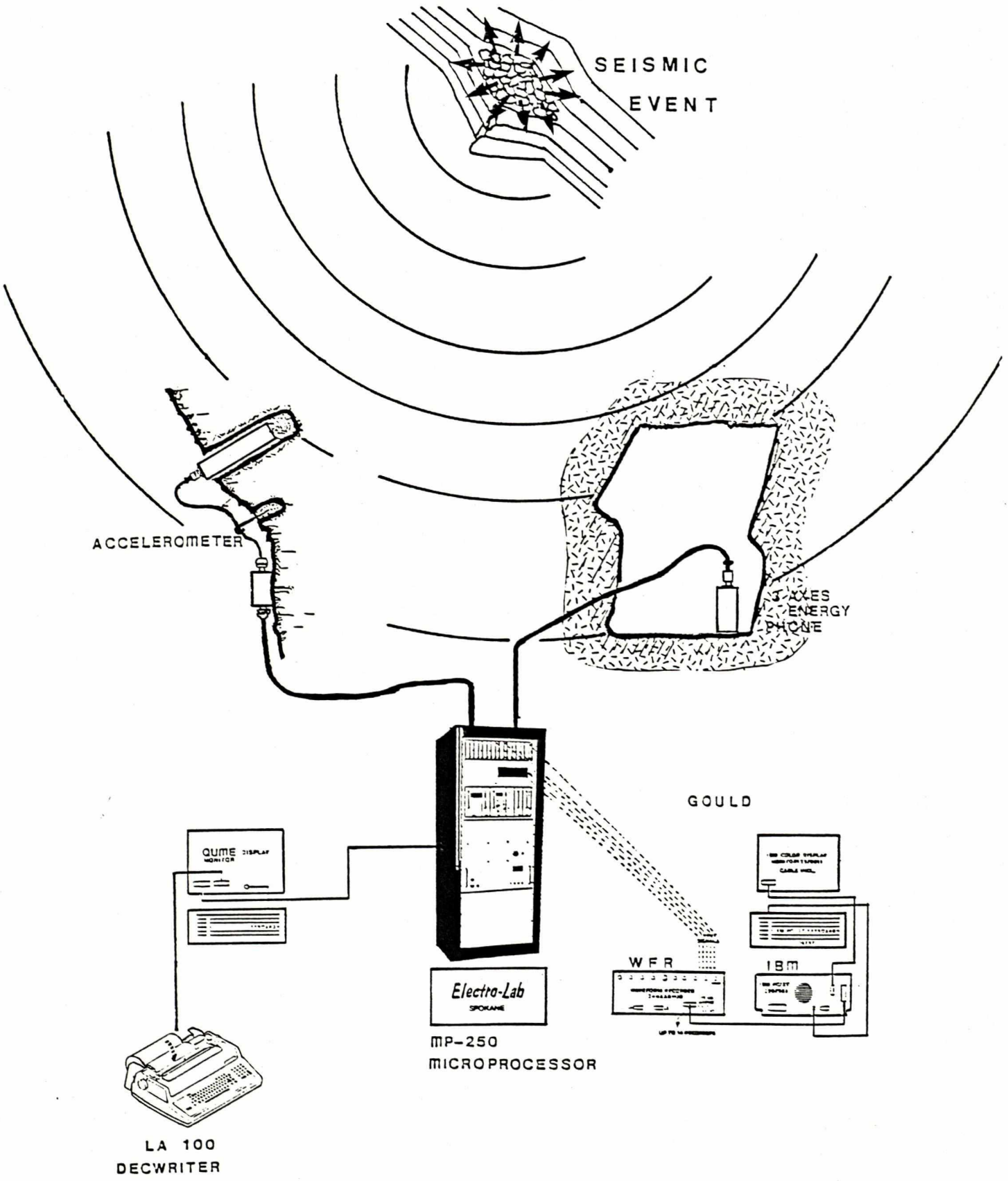

Fig. 6 - The microseismic data acquisition system.

device. The standard output device was the Qume (QVT-102) display monitor with the digitized signal relayed through the auxiliary port of the Qume to the LA-100 Decwriter having a 4 K storage buffer, for hardcopy printout.

Simultaneously, the Gould Dasa 9000 Data Acquisition and Retreival System recorded seismic data through the 250A filter interface located at the top of the Electro-Lab. Eight wire leads connected to the 250A filters via communication pins plugged into the front phone jacks were in turn connected to the 8-channel waveform recorder through triaxial BNC connectors attached at the back. The trigger channel of this recorder had a variably controlled threshold level as a percentage of the selected volts full scale sensitivity, which for all channels had a range capability of 0.05 to 500 volts. The analog signal received by the recorder was converted to digital form with transmission via an IEEE-488 interface to an IBM-PC/XT computer. The Gould Dasa 9000 software package allowed arming of the waveform recorder trigger with the auto-store to disc mode (recorder is armed, waits for a trigger, stores the event file then rearms), with the possibility of more than 200 (4K memory size) events if the former hard disc events were removed and transferred to floppies. The IBM-PC/XT was equipped with a TECMAR Graphics Card and IEEE card. Eight waveforms were visible via an IBM colour monitor display, and the software allowed amplification of a particular channel waveform for analysis and calculation purposes (area under the curve between specified points along the time axis).

The Gould waveform recorder had pre-selectable memory sizes per channel (2K, 4K, 8K, etc.) and with a low time base setting (low sample rate) a lengthy time window displaying the waveforms was possible. For the Macassa events a 4K memory was used and a time base setting sample rate of 1000 Hz resulted in a window time (excluding event pre-trigger) of approximately 500 milliseconds.

The Gould system allowed assessment of first motion studies, waveform characteristics and a means of checking the arrival time data displayed by the Electro-Lab MP-250.

GEOPHONE NETWORK

The geophone network (Figure 7) consisted of 12 model 271 accelerometers with a frequency range of 40-10,000 Hz and a sensitivity range of 250-500 volts/g (g is the gravitational acceleration, 9.8 m/sec^2). Power was supplied (36 VDC) to the accelerometers over two conductor wires from the 250 LA filters with the signal returning along the same wire. Eleven of the 12 accelerometers were located in the footwall with only geophone No. 2 residing in the hanging wall. Although accelerometers 11, 4, 12 and 6 define a reasonably spaced diamond shaped outer array limit in long section, a much reduced array thickness is shown in transverse section due mainly to limited hanging wall access. The initial feeling when deciding the geophone locations was that the events generated as a result of destressing the 58-40 crown pillar would initially be confined to the 58-40 crown pillar, and would progressively move towards the stope peripheries (58-40 and 57-40) where the ground would still be highly stressed but near critical strength levels.

The accelerometers were typically located 1.2 m above the footwall drift back in a near vertical position (44 mm hole) although the accelerometers could have been installed at any upward sloping orientation.

DESTRESS BLAST

REQUIREMENTS OF AN EFFECTIVE DESIGN

In designing a destress blast, four major areas must be satisfied:

1) The spacing, size, and length of the destress holes should be sufficient to cause effective fracturing of the intact highly stressed rock (the central core of the crown pillar).

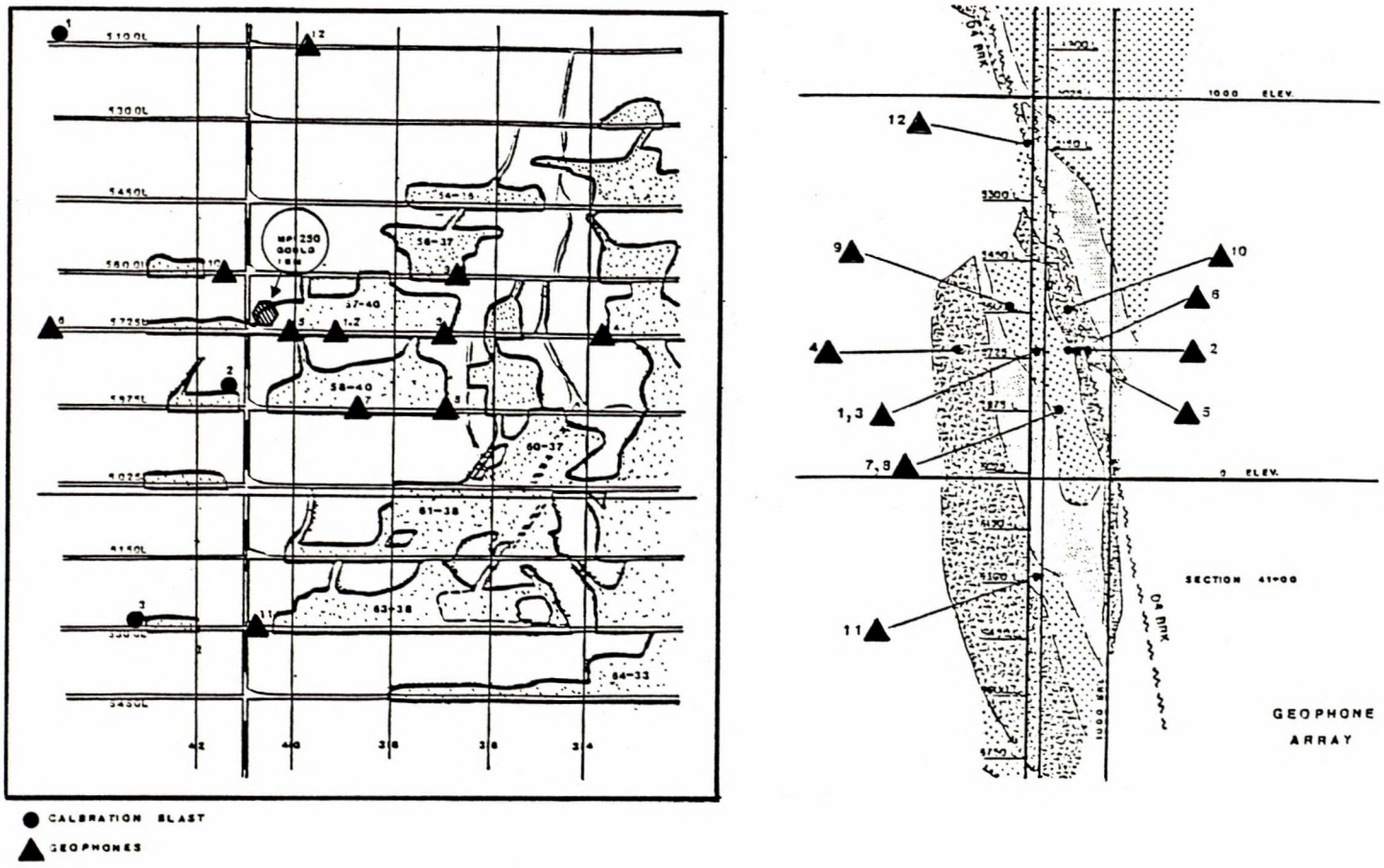

Fig. 7 - Geophone layout for monitoring the destress blast in longitudinal, transverse and composite plan views.

2) The blast should not generate excessive peak particle velocities resulting in damage to the other structures outside the immediate area to be destressed.
3) An adequate monitoring program should be in place to verify the 'before' and 'after' site conditions where destressing is to be attempted. Hopefully, the changed site conditions are evaluated through independent instrumentation programs (tape convergence and microseismic), but that the observations and conclusions from these different reconnaisance methods correlate well.
4) Extensive thought should be given to the timing of the destress blast both from a mining sequence framework and blast scheduling. Verification that destressing a crown pillar will not cause a multiple succession of crown pillar failures (domino effect) is crucial.

If an existing calibrated computer mining simulation model exists, then modelling of the current mine geometry simulating the destress blast (before it happens) can be used to verify the extent of induced failure as a result of the destress blast. If only localized failure is induced (by comparing the amount of failure before and after destress simulation), then this suggests that destress blasting will cause little deterioration to the other workings.

A further recommendation for future destressing attempts is to compare underground convergence and stress changes measured with the actual computer model's predictions. If the model is reasonably well calibrated, these results should be comparable. Disagreement may suggest (if no convergence is measured near a destressed crown pillar but the computer model suggests there should be) that a localized portion of the pillar may still be intact and highly stressed, or that the instrumentation was not properly coupled to the elastic portion of the rock mass. If adequately coupled this would suggest a further potential for bursting and that further localized destressing (long

hole blasting) is required.

The destress blast should be fired during a weekend to give the destressed rock a chance to fully converge and induced bursts to occur with no personnel around.

BLAST DESIGN CONCEIVED

1) The destress holes in the 58-40 crown pillar, 14 in total (drilled by bar and arm set-up) had a diameter of 63.5 mm,average spacing of 3.0 m, orientated at $+55^{o}$ East, length 16.8 m and were located within the footwall of the '04' Break (Figure 8).
2) The holes were to be loaded with ANFO from the toe to the start of the fractured zone where barite stemming from Ground Control (Sudbury), or inert gel from CIL was placed to occupy the first 3.6 m from the hole collar.
3) The holes were designed with a prescribed powder factor of 0.05 kg/tonne initiated with nonel millisecond delays (starting at 25 ms and increasing) resulting in 42.2 kg/delay.
4) Precalculated peak particle velocities indicated 45.7 cm/sec for the stope, and 20.3 cm/sec for the 58-36 ore pass, and Macassa's rock mechanics group experience was that 25.4 cm/sec would result in minimal damage to the underground workings at this location. The use of stemming insured that the low powder factor confined the blast energy to fracturing the intact rock efficiently.

Drilling of the destress holes did meet with some difficulty due to squeezing ground, and there was general concern whether this destress blast might trigger bursting elsewhere in neighbouring openings. Examination of the existing mine geometry in the No. 3 shaft area and observed ground conditions to date suggested that most of the failure induced by the destress blast would be confined to the immediate area. Application of the NFOLD displacement

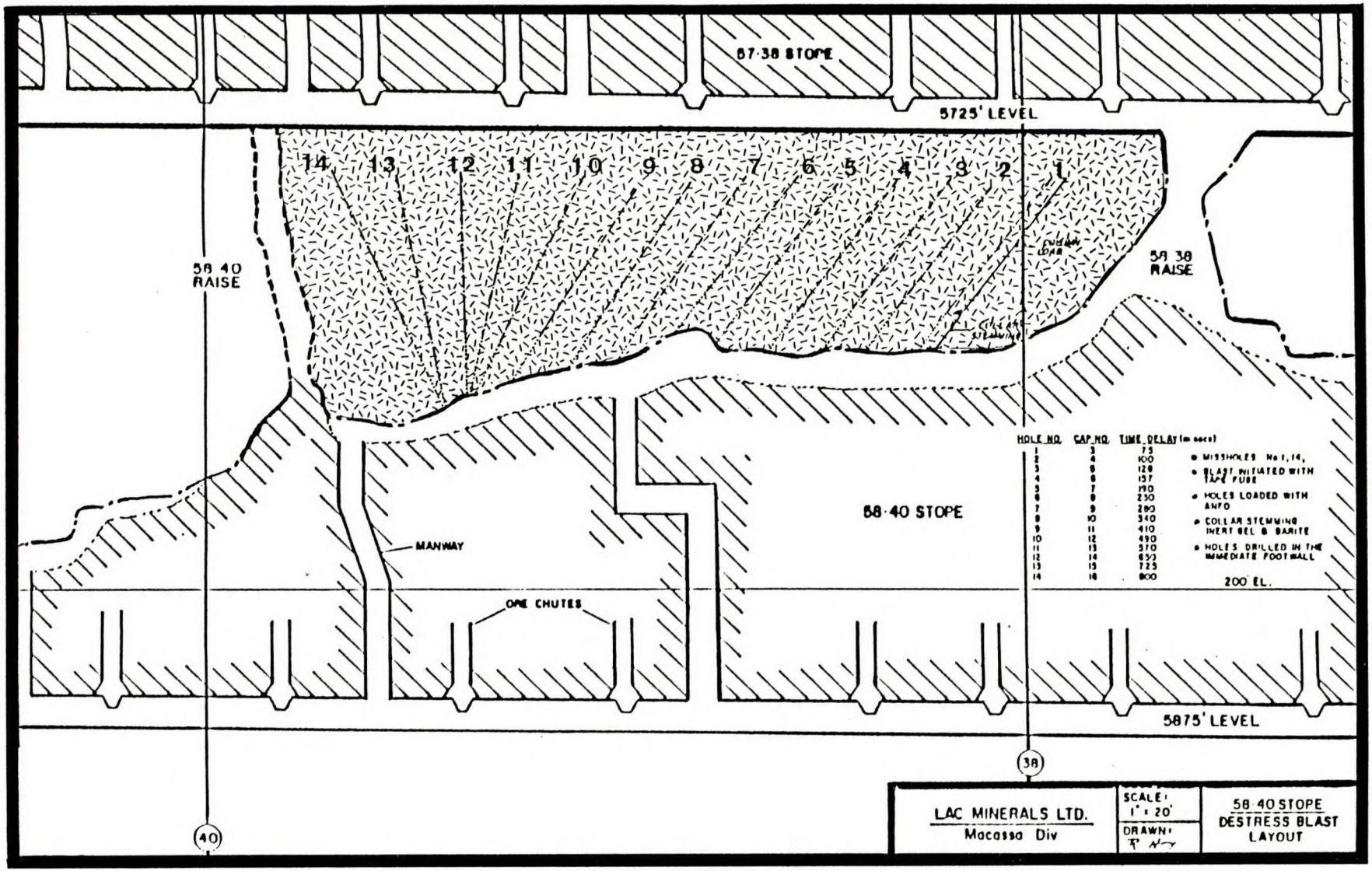

Fig. 8 - Destress blast specifications.

discontinuity destress simulation model later verified this to be the case.

The destress blast was fired on June 28, 1986, Saturday, at 12:03 a.m. at the start of the Canada Day long weekend which would give the ground near the 58-40 crown pillar a long enough time buffer to yield before personnel would have to enter the area.

SUCCESS OF THE DESIGN BLASTING RESULTS

Of the 14 holes that were to be included as part of the destress blast (Figure 8), hole No. 1 could not be loaded properly, and hole No. 14 was not initiated properly and appeared to misfire as was first observed through the Gould waveform analysis equipment, and later through close inspection within the stope back. The designed column loads could not be achieved as hole diameters had squeezed, resulting in a powder factor of 0.03 kg/tonne.

The hole collars were not stemmed as designed due to squeezing ground resulting in CIL inert gel being inserted (3.0 m) followed by a smaller quantity of barite.

Some cratering of the collars occurred in the central area of the blast where inadequate stemming was present, but the degree of cratering could also have been assisted by advanced pre-fracturing from earlier blasting.

Blast vibration damage was non-existent within the 58-38 ore pass or the 5725 level directly above the 58-40 crown pillar. Also, there appeared to be no secondary bursting occurring in the pillar while it was being examined during the following week.

The rock mechanics department decided to obtain a better, visual inspection of the blasted pillar's 'central core'. This was achieved by diamond drilling at a location between destress holes 12 and 13, and where the hole intersected the plane of the destress holes the core was extremely fractured (Figure 9). On either side of this intersection no discing of the core was observed and a much higher RQD was obtained.

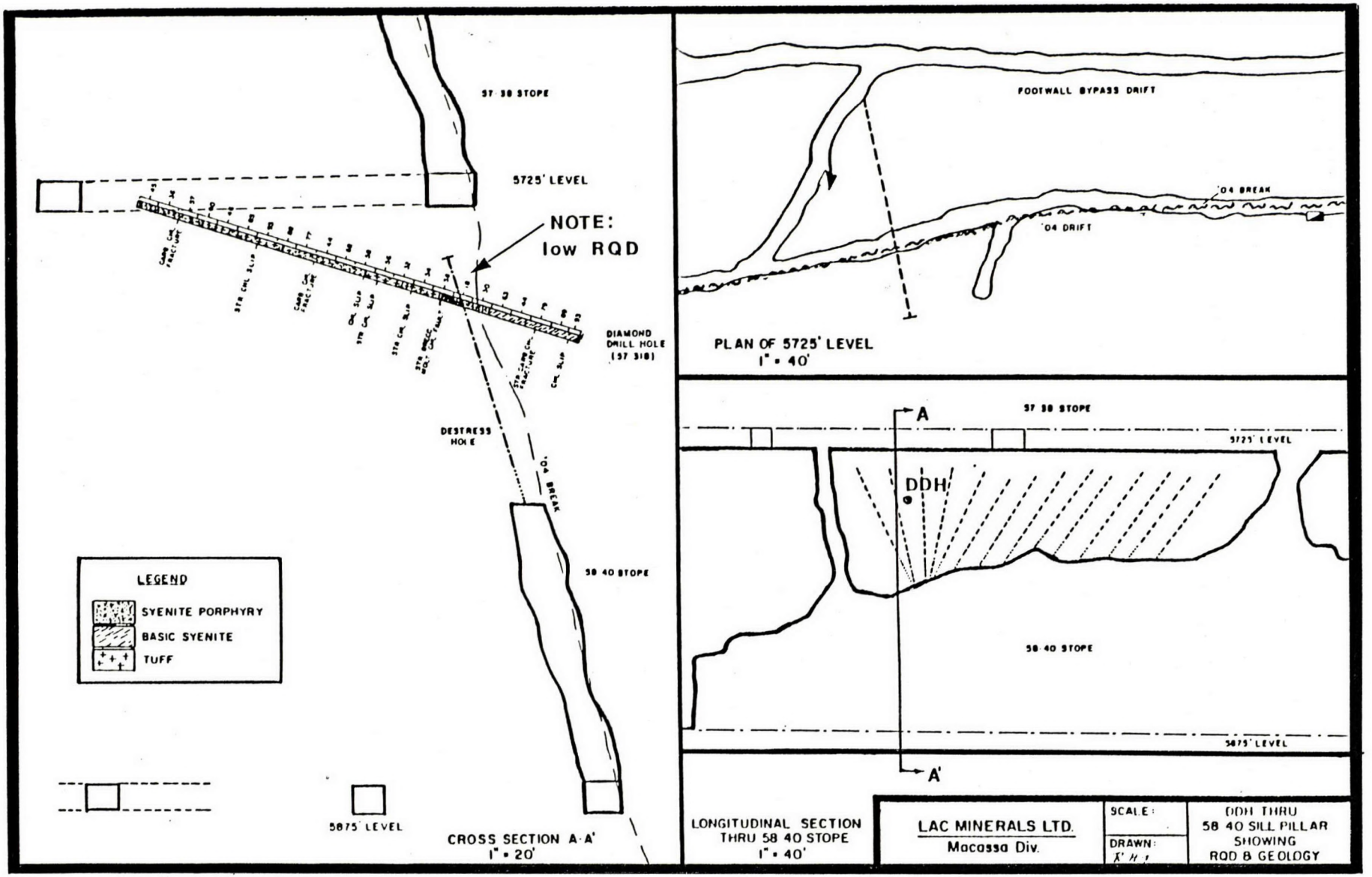

Fig. 9 - Destress blast fracturing assessment through core logging.

TAPE CONVERGENCE MONITORING RESULTS

The actual measured convergence for each of the tape extensometer points is shown in Table 3 with the overall trends described below:

1) The maximum convergence appeared to occur in the western part of the upper 58-40 stope (lower western 58-40 crown portion). Pin 58.5 had a net convergence of 1.12 in (28.5 mm) while pins 58.2 to 58.5 averaged 0.81 in (20.5 mm).
2) Pin 58.1, however, had a net convergence of only 0.24 in (6 mm), but it was noted that the No. 1 hole in the same vicinity had not been loaded.
3) In general, it appeared that substantial convergence had occurred for two-thirds of the western strike length of the crown pillar with the remaining eastern third still not fully converged.
4) Very minimal convergence occurred along the 5725 level convergence pin locations (1A,1B → 10A,10B) following the blast and for a considerable period thereafter.

For the most part it was felt that the destress blast had been a success as fairly significant convergence had occurred throughout most of the 58-40 stope.

MICROSEISMIC ACTIVITY AS A RESULT OF THE DESTRESS BLAST

Three source location methods (Direct, Block. Simplex solutions) were applied to analyze the event arrival time data following the 58-40 crown pillar destress blast (June 28, 1986, 12:03 a.m.). Figure 10 and Appendix A display the results in both transverse and longitudinal sections. Details of the Simplex source location solutions as defined by event size are demonstrated in Figure 10. All source location algorithms produced a cluster of events within the central and lower 58-40 crown pillar and upper 58-40 stope. The top portion of the 58-40 crown pillar was void of activity as was the eastern one-third section. There was very little activity generated above

Table 3 - Convergence Measurements, 58-40 Crown Pillar
before and after destressing

*********Lac Minerals/Macassa Division**********

Closure Measurement for the 5725 Level

Date	1A	1B	2A	2B	3A	3B	4A	4B	5A	5B	6A	6B	7A	7B	8A	8B	9A	9B	10A	10B
21/04/86	0.00	0.00	0.00	0.00	0.00	0.00	0.00	0.00	0.00	0.00	0.00	0.00	0.00	0.00	0.00	0.00	0.00	0.00	0.00	0.00
30/04/86	-0.07	-0.17	0.17	0.02	-0.14	0.08	-0.47	0.17	-0.16	-0.03	-0.74	0.17	-0.10	0.36	0.29	0.40	-0.60	0.46	0.40	0.48
07/05/86	-0.05	0.02	0.36	0.19	-0.21	-0.05	-0.32	0.18	0.10	0.05	-0.16	0.15	0.14	0.33	0.23	0.37	0.04	0.52	0.51	0.32
15/05/86	-0.21	-0.33	0.16	0.23	-0.01	0.24	-0.49	-0.63	-0.62	0.02	-0.12	-0.09	-0.08	0.14	0.23	0.44	0.65	0.73	0.53	0.55
21/05/86	0.11	0.05	0.26	0.40	-0.03	0.10	-0.35	-0.18	-0.63	-0.08	-0.12	-0.14	-0.05	0.11	0.07	0.29	0.38	0.44	0.38	0.58
18/06/86	-0.38	-0.21	-0.36	-0.14	-0.47	-0.54	-1.01	-0.65	-1.10	-0.62	-0.51	-0.25	-0.45	-0.18	-0.10	0.08	-0.23	-0.50	10.47	0.11
26/06/86	-0.37	-0.39	0.01	-0.08	-0.67	-0.69	-1.42	-1.30	-0.49	-0.85	-0.91	-0.91	-0.34	-0.19	-0.31	-0.11	-0.45	-0.54	0.17	-0.17
27/06/86																				
01/07/86	-0.51	-0.54	-0.33	-0.06	-0.96	-1.00	-1.80	-1.65	-1.73	-1.34	-4.01	-4.24	-26.57	-1.97	-1.37	-1.65	-0.77	-1.33	0.25	-0.11
09/07/86	-0.38	-0.51	0.07	0.02	-0.74	-0.90	-2.20	-1.78	-1.60	-1.38	-4.67	-4.60	-51.71	-2.01	-1.62	-1.78	-0.98	-1.30	-0.05	-0.35
30/07/86	-0.52	-0.54	-0.25	-0.36	-1.12	-1.57	-2.60	-2.80	-2.13	-1.93	-5.00	-5.28	-52.17	-2.71	-1.93	-2.00	-1.43	-1.77	-0.18	-0.46

Remarks: 1. Destress holes blasted in 58-40 stope on June28,1986.
2. "A" = 6 ft. pin
3. "B" = 2 ft. pin
4. Closure measurement in millimeters

Closure Measurement for the 58-40 Stope

Date	1	2	3	4	5
16/06/86	0	0	0	0	0
23/06/86	0	0	0	0	0
01/07/86	-5.57	-14.37	-22.06	-16.36	-28.18
08/07/86	-5.94	-14.73	-22.56	-17.19	-28.44
30/07/86	-6.50	-15.29	-22.62	-17.73	-28.85

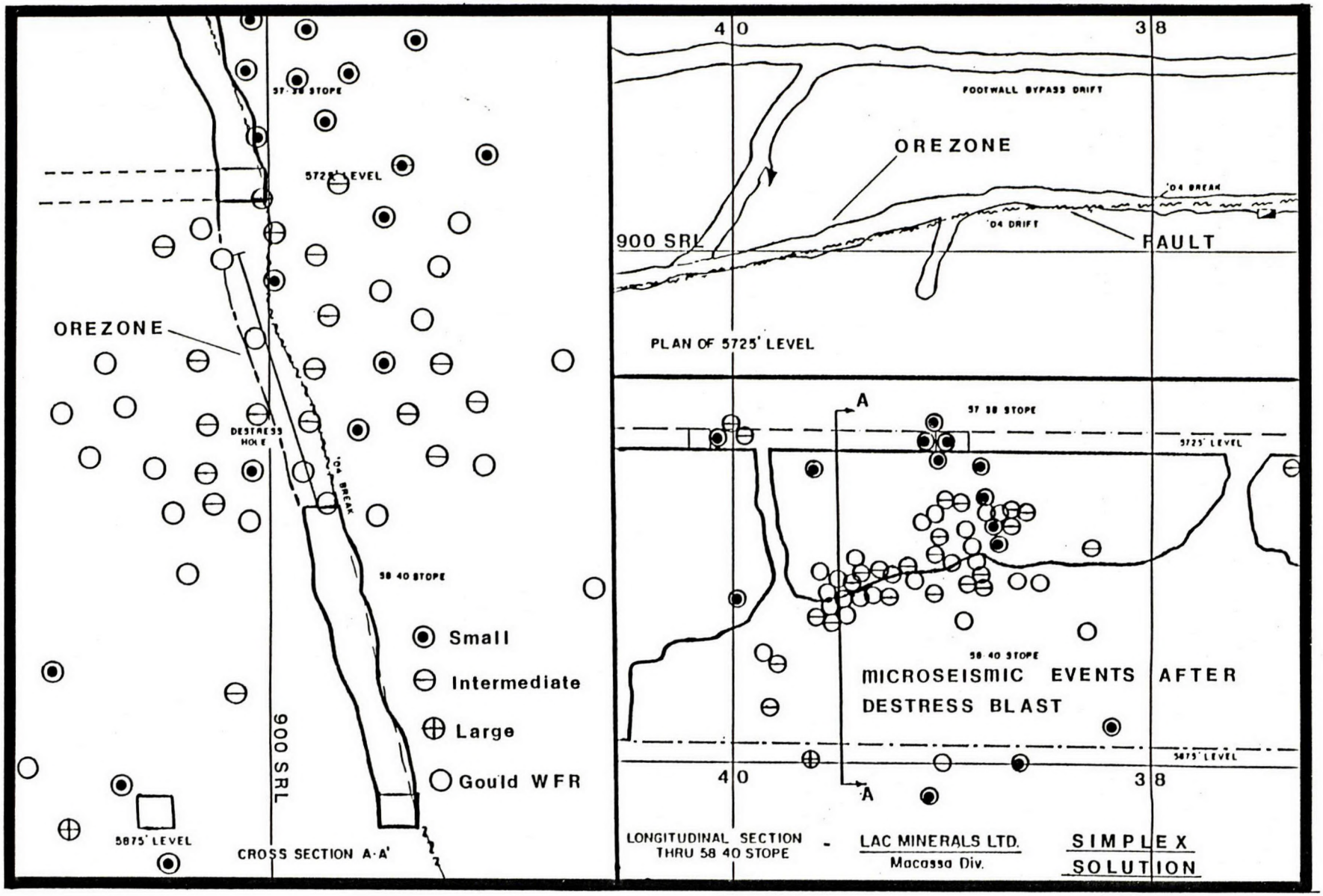

Fig. 10 - Microseismic event source locations generated by the destress blast - Simplex solution.

the 5725 level, with only an isolated spattering of events confined to the large pillar below the 5875 level.

The microseismic activity after the destress blast suggested that:

1) The upper portion of the 58-40 crown pillar was already destressed prior to the June 28, 1986 destress blast, or that the destress blast as designed left a narrow intact zone (assumed to be fractured) just below the 5725 sill elevation still intact, but highly stressed.
2) Approximately two-thirds of the 58-40 crown pillar was successfully destressed (western and central portions) except for the eastern section and possibly just below the 5725 level.
3) Seismic events were generated only in the immediate vicinity of the 58-40 crown pillar, and nowhere else in the mine, reflecting adequate buttressing pillars.
4) Most events were clustered within the ore seam.

The categorization of the event magnitude was according to the following criteria:

Event Size	Electro-Lab MP-250 Energy Number	No. of Geophones Hit
Small	<5000	<8
Intermediate	5000-9999	8-11
Large	>9999	12

Of the 234 events examined following the destress blast, 72 were plotted. The event sizes categorized by percent frequency population were as follows:

Event Classification	% Frequency
Small	25
Intermediate	11
Large	0.5
Gould (WFR)	62

Some 19 min after the destress blast (12:03 a.m.) a malfunction of the LA-100 decwriter occurred (12:22.48 a.m.) as high humidity conditions and temperature had adversely weakened the printer paper. The frequency distribution therefore was more heavily weighted with Gould data.

Energy calculations were not performed on the Gould accelerometer waveforms as it was difficult to correlate the results with the Electro-Lab MP-250 energy units.

At 3:22 a.m., the Gould IBM-XT hard disk was full, and with the Auto-Store-to-Disk mode inoperable, the result was a period of 4 h 8 min where no data were captured until the LA-100 was reactivated at 7:30 a.m., and the Gould hard disc data files were down loaded to floppy diskettes to free up hard disk memory.

Earlier attempts to route the Electro-Lab MP-250 digitized data via GANDOLF modems utilizing 4 isolated wires contained within multiwire shaft cable had failed as the modems could not be properly set. Had the modems functioned properly the LA-100 decwriter would have been able to operate under a controlled temperature and humidity environment within the new office complex on surface, and considerably more data obtained from events triggered by the destress blast.

The clustering of microseismic data suggested that a successful destress blast had been completed on the 58-40 crown pillar and that it had not triggered rockbursts other than in the immediate destress area to a large

extent.

COMPUTER MINING SIMULATION

MODEL CALIBRATION

Both the elastic DZTAB, elastic and non-linear post failure NFOLD 3-dimensional displacement discontinuity stress and displacement analytical methods were used by CANMET to model the No. 3 shaft mining area.

Rectangular elements are established to simulate mined and unmined sections within a tabular orebody where the orebody thickness is small in relation to its other dimensions.

Elastic analysis is usually completed on the mining area of influence to simulate stress conditions at an extraction geometry where failure begins. Non-linear post-failure analysis is then carried out on the same geometry until the non-linear model is 'fine tuned' to the point where the predicted model failure areas agree with the observed failure within the mined orebody. Model calibration in this case is very dependent on accurate observations by the mine's rock mechanics staff and good documentation of the same. Once the model is calibrated future mined outlines can be evaluated, or as in this case, a crown pillar destress simulation modelled.

Design of the No. 3 shaft pillar involved earlier elastic analysis using the NFOLD model by Golder Associates of Toronto. Discussions with them revealed that their model consisted of a coarse element size (12.2 m x 12.2 m), resulting in 2500 elements, and was the maximum size that could be comfortably run on their IBM-AT. CANMET wished to use a much smaller element size (3.05 m x 3.05 m), to model a mine geometry inclusive of the 58-40 crown pillar which would generate 7000 elements. As a result, the CANMET NFOLD models (elastic and non-linear) were run on Boeing's Cray Supercomputer in Seattle, Washington.

The input parameters for the initial elastic and restart non-linear models are shown in Tables 4 and 5. These Tables show that the physical model dimensions are constructed along with the inclusion of cell dimensions, primitive stress components, elastic modulus and Poisson's Ratio for the rock mass, as well as seam material properties. In this model a mining pattern is created and stresses are imposed on this pattern.

The non-linear post failure analysis (Table 6) shows more complex input data requirements. Post failure elements are incorporated in the mined geometry at the onset of failure with various load-deformation properties assigned to the elements according to their degree of confinement. The purpose is to simulate actual failure underground under high stress loading where the weaker less confined elements fail and transfer load to the stronger more confined elements.

Since the elastic NFOLD analysis doesn't allow failure to occur, backfill elements and their properties are only introduced in the non-linear post-failure model where some load is held by the backfill as well.

Once the non-linear post failure analysis model has been calibrated by fine adjustments in the yielding elements peak and residual strengths so that 'predicted' equals 'observed' failure for a given mine geometry, this model can also be used to simulate a destress blast.

If a particular crown pillar is to be destressed the model simulation involves picking those elements that will be affected and decreasing their peak and residual strengths so that they are marginally less than, or equal to, the lowest stress conditions present in the pillar just prior to destressing. Although it is known that destressing results in a reduced elastic modulus and failure of formerly highly stressed elements, CANMET's experience with the NFOLD model indicates that reducing the peak and residual strengths generally accounts for most of the convergence and stress changes

Table 4 - Elastic NFOLD model input parameters

GEOMETRY

No. of Joints (on Strike)	No. of Limbs (down dip)	Max Limbs/Fold	No. of Folds	Starting Fold Coordinates (X,Z plane), m		Dip°
				X	Z	
14	20	5	4	0.0	1614.0	72
				25.75	1690.2	
				49.52	1766.4	
Total elements = 14 x 20 x 25 = 7000				74.27	1842.2	

STRESSES

General Form:
σ_{XX} = AXX + BXX.Z (depth in metres), etc.
σ_{XY} = AXY + BXY.Z (depth in metres), etc.

AXX = AYY = AZZ = 0
AXY = AYZ = AZX = 0

BXX = 0.044 MPa/m
BYY = 0.034 MPa/m
BZZ = 0.028 MPa/m
BXY = 0.006 MPa/m
BYZ = -0.003 MPa/m
BXZ = -0.002 MPa/m

MATERIAL PROPERTIES

Elastic Modulus 59,310 MPa
Poisson's Ratio 0.2

Unmined material property I.D.	2
Thickness	2.40 m
Elastic Modulus	59,310 MPa
Poisson's Ratio	0.2
Normal Stiffness	24,712.5 MPa/m
Shear Stiffness	10,246.9 MPa/m

* Note: No backfill properties entered here.

Table 5 - Non-linear, post-failure NFOLD input parameters (assuming restart from elastic run)

Similar to elastic run except:

1) Some elastic elements are reassigned both pre- and post-failure load deformation properties;
2) Some mined elements are replaced with backfill elements;
3) Assignment of element strengths based on degree of actual failure observed (i.e., crown pillar) with adjustments to strengths so stress/strength $\geq$1.0 at failure locations only;
4) Stress environment not changed;
5) Overall geometry remains unchanged.

Material Property No.	Seam Thickness (m)	Deformation Modulus (MPa)	Poisson's Ratio	Unmined Elements: Post Peak Modulus (MPa)	Yield Strength (MPa)	Residual Strength (MPa)	Cohesion (MPa)	Internal Friction (degrees)
2	2.4	59310.0	0.2	(Elastic Element)				
12	2.4	59310.0	0.2	19970.0	140.0	60.0	50.0	60.0
22	2.4	59310.0	0.2	19970.0	140.0	70.0	50.0	60.0
32	2.4	59310.0	0.2	19970.0	165.0	100.0	50.0	60.0
42	2.4	59310.0	0.2	19970.0	175.0	140.0	50.0	60.0
52	2.4	59310.0	0.2	19970.0	185.0	160.0	50.0	60.0
62	2.4	59310.0	0.2	19970.0	195.0	185.0	50.0	60.0

Material Property No.	Backfill Elements: Convergence After Fill (Elastic Run) (m)	Primary Fill Stiffness (Field Data) (MPa/m)	Wall Convergence Before Fill Pressurizes (m)	Convergence Up To Next Stiffness Inflection (m)	Secondary Fill Stiffness (Field Data) (MPa/m)
-6	0.06	75.0	0.0	0.05	150.0
-5	0.05	75.0	0.0	0.04	150.0
-4	0.04	70.0	0.0	0.04	140.0
-3	0.04	70.0	0.0	0.03	140.0
-2	0.03	65.0	0.0	0.02	130.0
-1	0.02	65.0	0.0	0.02	130.0

measured in situ. Reducing the elastic modulus does not seem to provide a very significant contribution.

The 58-40 crown pillar was analyzed as the focal point throughout the elastic, non-linear post-failure, and destress simulations.

Close inspection within the elastic analysis revealed that elements with perpendicular stresses greater than 145 MPa corresponded well with those areas where failure was observed in the mine. Figure 11 shows the mining pattern layout for the elastic case, and Figure 12 shows the perpendicular stresses generated as a result. Figure 12 diagramatically shows those areas flagged as having failed if 145 MPa is used as the criterion. Closer inspection of the 58-40 pillar demonstrates that the 145 MPa failure criterion correlates well with the fractured zone defined through diamond drilling.

To accurately simulate the degree of failure within the NFOLD model the non-linear load-deformational properties as defined earlier were assigned according to the mining pattern in Figure 13. Basically, the weaker elements are located where they are fully exposed or have a very small confining stress at right angles (within the seam) to the perpendicular stress. These areas typically are the edges of pillars or stope openings only a small distance into the rock mass. Within the mining pattern there also exists a backfill element pattern which has a direct correlation with the amount of stope convergence having occurred, as determined from the earlier elastic analysis.

Figures 14 and 15 demonstrate the degree of failure for the calibrated load-deformation properties and show the perpendicular stress levels expected for the various unmined elements. Typically, residual stress conditions are present where the factors of safety are less than unity, and immediate to these areas very highly stressed elements with factors of safety slightly greater than, or equal to, unity are common. Close examination of the 58-40 crown pillar shows this by example. Figure 15 demonstrates the possibility of

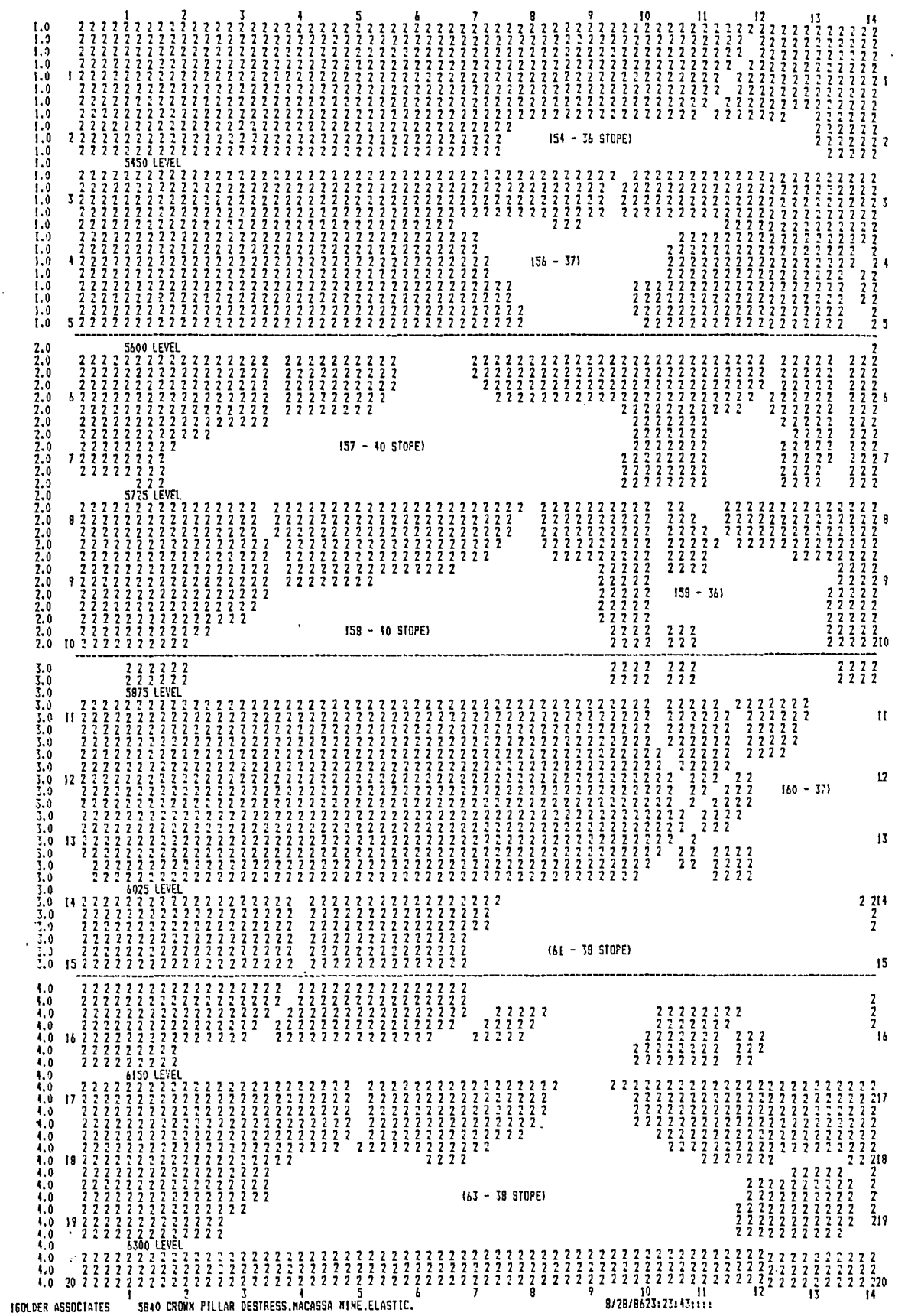

Fig. 11 - Mining pattern layout of Macassa Mine for the No. 3 shaft area, elastic analysis.

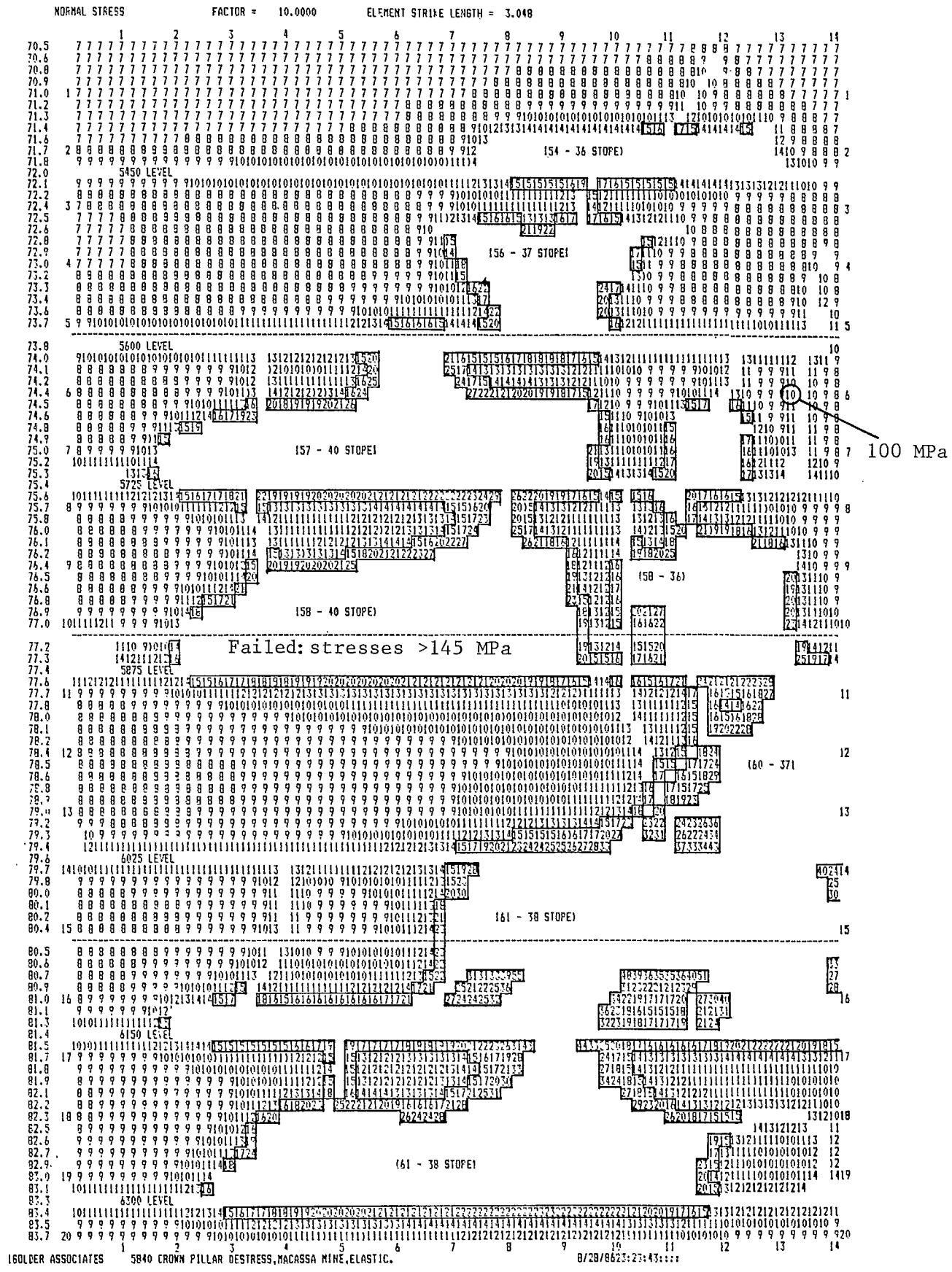

Fig. 12 - Perpendicular stress levels and demarked failure areas, elastic analysis.

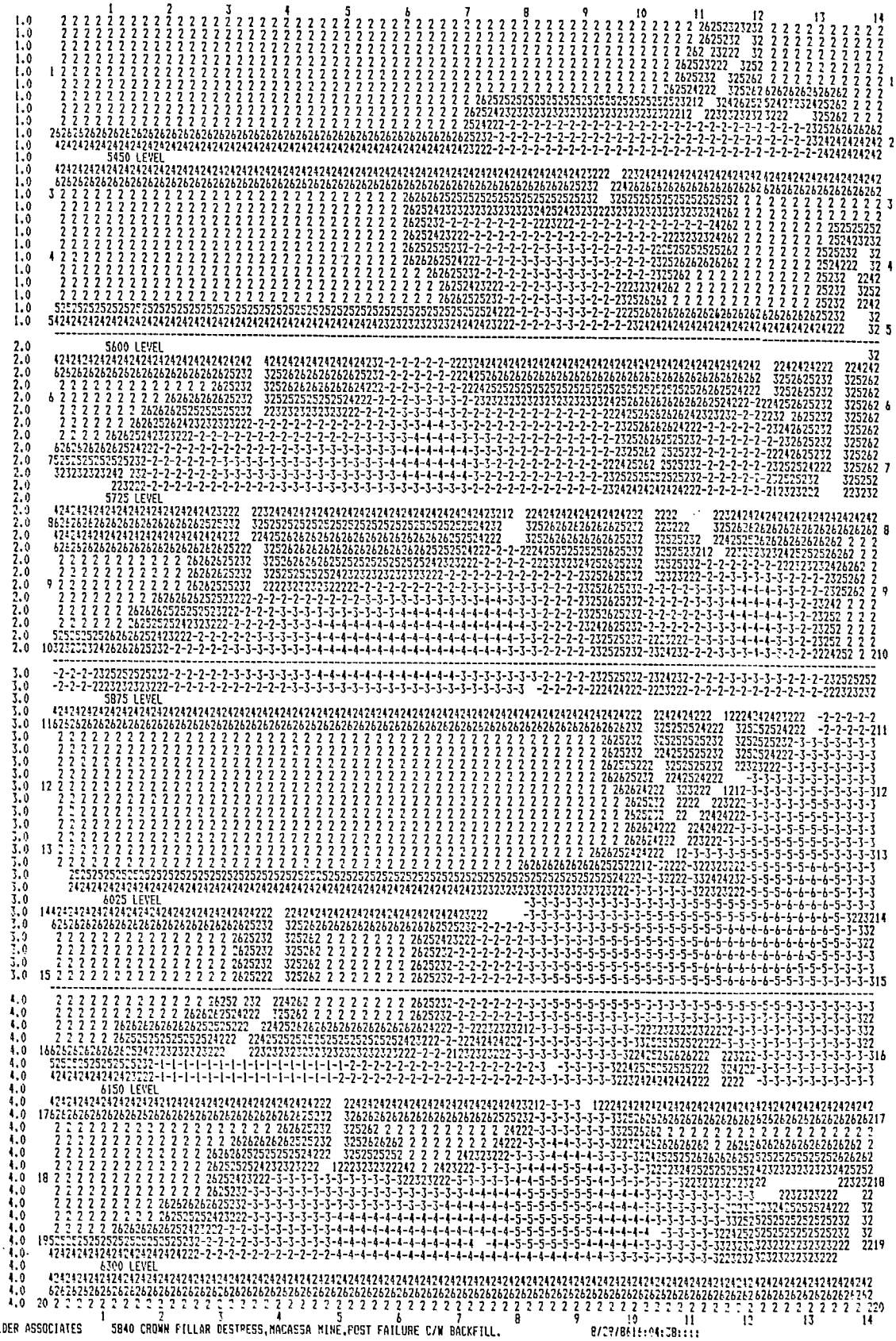

Fig. 13 - Mining pattern with assigned elastic and non-linear post-failure element properties.

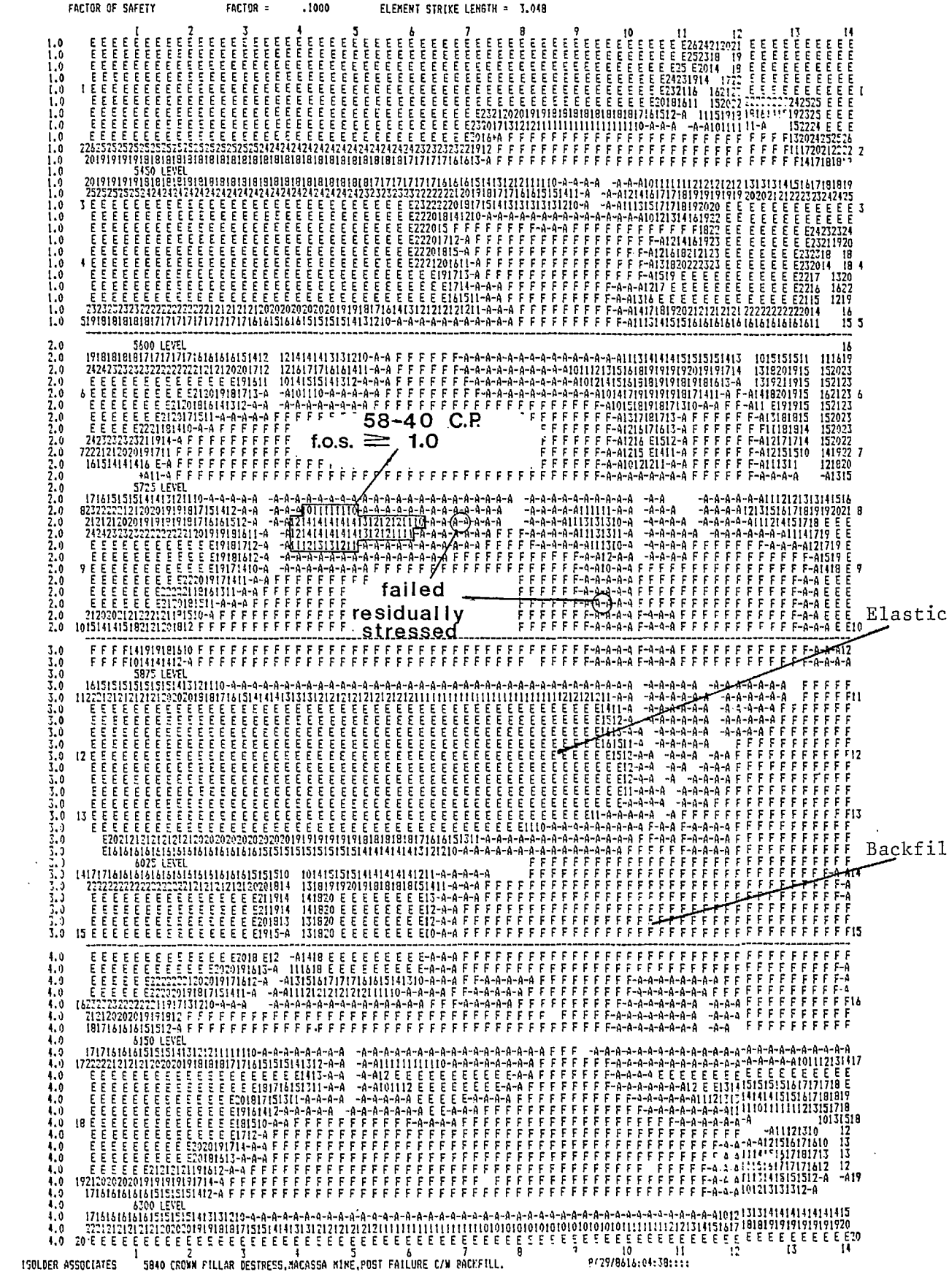

Fig. 14 - Strength/stress ratios for non-linear model incorporating yielding elements.

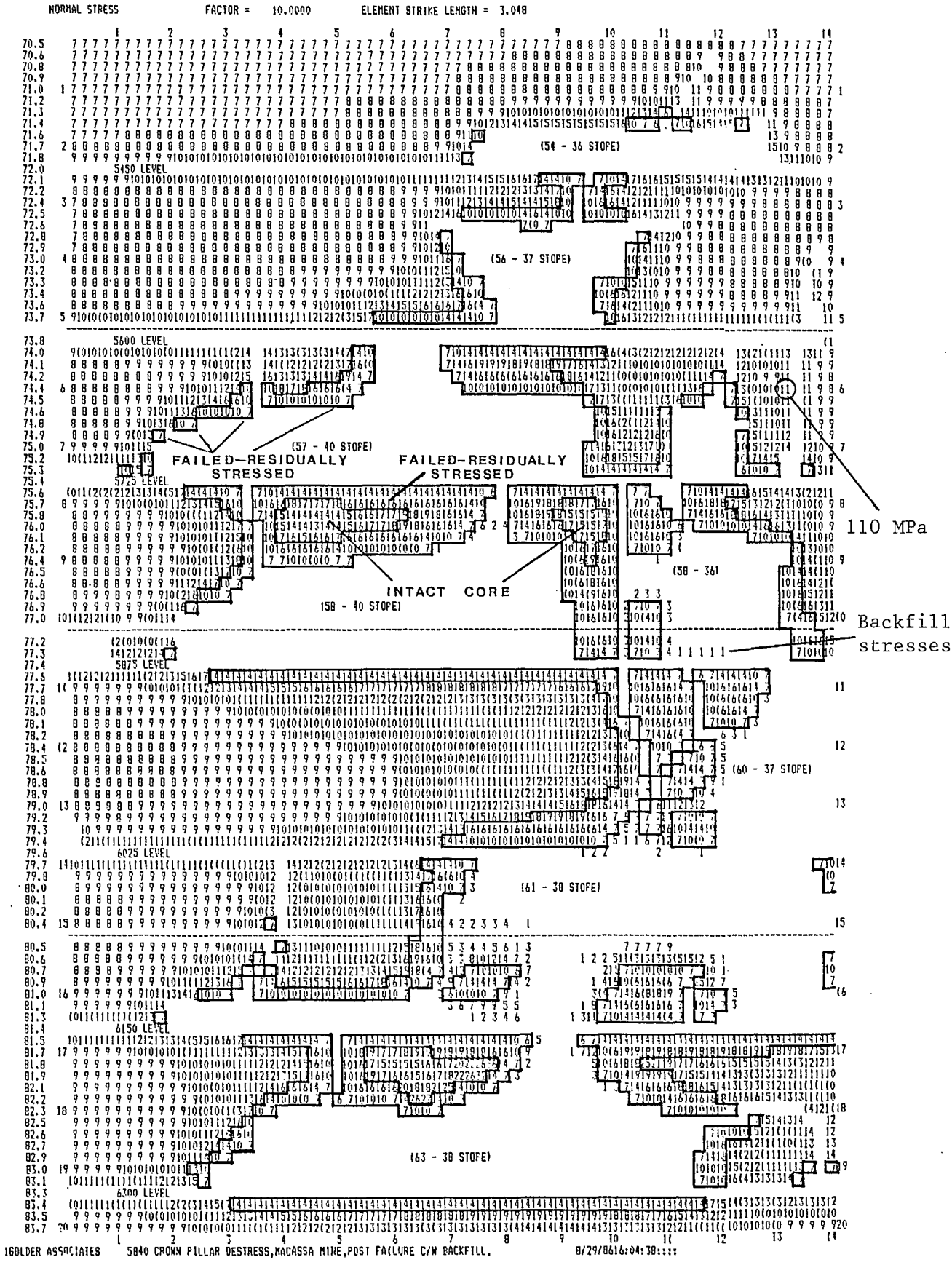

Fig. 15 - Perpendicular stresses with failed regions displayed (non-linear model).

failed elements near the inner core having higher stresses than the stronger intact core elements. This suggests triaxial loading conditions near the pillar centre and uniaxial loading conditions at the pillar edges. The central core of elements are highly stressed, but the core is much smaller than for the earlier elastic case. Attempts were made to adjust the peak and residual strengths higher, but significant increases to anomalously high values were necessary to generate a larger intact pillar core.

It should also be noted in examining the perpendicular stress results (Figure 15) that where failure of the unmined elements is fairly extensive (west of the 60-37 stope, bottom 61-38 stope, upper 63-38 stope) significant stress transfer to the backfilled elements has occurred. Although this has not been verified through pressure meters installed in the backfill, the narrow stope width and angular mined waste development would most likely adequately support this stress transfer.

The rock mechanics department of the Macassa Division verified that the degree of failure witnessed elsewhere in the non-linear post-failure NFOLD model matched the degree of ground deterioration. Specific examples are the 57-40, 57-38 crown pillar buttresses just below the 5600 level, the 36-waste pillar separating the 58-40, 57-40 and 58-36 cut-and-fill stopes, the western outline of the 58-40 stope, and the absence of failure on the large buttress pillar separating the 5875 and 6025 levels.

DESTRESS SIMULATION

Simulation of the destress blast was accomplished by a gradual lowering of the 58-40 crown pillar element strengths. This meant lowering the peak and residual strengths slightly, running the model to determine if crown pillar failure occurred, and comparing the differential convergence generated from the simulation with the differential convergence measured from the actual pre-blast tape extensometer results.

Several trial runs were completed until the 58-40 crown pillar had failed completely and the convergence differential obtained compared favourably with the underground measurements.

Table 6 demonstrates the input parameters used for the destress simulation and the final assignments given to the peak and residual strengths after several trial runs.

Figure 16 shows the mining pattern with the 58-40 crown pillar now composed of newly assigned material reference numbered elements. The material strength properties for elements at other locations has remained unchanged.

Figure 17 indicates complete failure of the 58-40 crown pillar which would be the case if the pillar was successfully fractured by the destress blast.

The former NFOLD analyses containing post-failure criteria and an indication of the extent of failure within the 58-40 crown pillar and its surroundings prior to the destress blast were matched against the extent of failure generated from the destress simulation. Very little additional failure was generated in the surroundings (Figure 17) other than the crown pillar.

Only a few additional elements failed within the central core of the 36-waste pillar, the western outline of the 58-40 stope, and the western upper crown pillar buttress of 57-40 stope. None of the other locations in the mine were affected by the destress blast simulation. Limited spans and the degree of extraction were more than likely instrumental in suppressing the effects of the blast. Figure 18 displays the stress conditions as a result of the destress simulation.

Just as the numerical analysis was used to compare the differential failure areas before and after the destress simulation, the convergence before and after the destress simulation was compared as well. Figure 19 shows the effect of the destress simulation and the increased convergence as expected.

Table 6 - NFOLD input parameters - destress simulation.

Similar to non-linear post-failure analysis except:

1) New element properties assigned to 58-40 crown pillar elements;
   - these have lower yield and residual strengths so that they will deliberately fail;
   - strengths defined through trial and error (1) iteration runs comparing predicted model convergence change from former non-linear run to destress simulation run, with actual convergence change measured underground after blast.
2) Element properties at all other locations within the former post-failure model remain unchanged (fill elements also);
3) Overall geometry remains unchanged;
4) Stress environment unchanged.

Material Property No.	Seam Thickness (m)	Deformation Modulus (MPa)	Poisson's Ratio	Post Peak Modulus (MPa)	Yield Strength (MPa)	Residual Strength (MPa)	Cohesion (MPa)	Internal Friction (degrees)	
11	2.4	59,310.0	0.2	19,970.0	100.0	70.0	30.0	60.0	
21	2.4	59,310.0	0.2	19,970.0	100.0	80.0	30.0	60.0	
31	2.4	59,310.0	0.2	19,970.0	100.0	90.0	30.0	60.0	Destressed
41	2.4	59,310.0	0.2	19,970.0	100.0	100.0	30.0	60.0	Elements
51	2.4	59,310.0	0.2	19,970.0	100.0	100.0	30.0	60.0	58-40 C.P
61	2.4	59,310.0	0.2	19,970.0	100.0	100.0	30.0	60.0	
12	2.4	59,310.0	0.2	19,970.0	140.0	60.0	50.0	60.0	
22	2.4	59,310.0	0.2	19,970.0	140.0	70.0	50.0	60.0	Remaining
32	2.4	59,310.0	0.2	19,970.0	165.0	100.0	50.0	60.0	Unmined
42	2.4	59,310.0	0.2	19,970.0	175.0	140.0	50.0	60.0	
52	2.4	59,310.0	0.2	19,970.0	185.0	160.0	50.0	60.0	
62	2.4	59,310.0	0.2	19,970.0	195.0	185.0	50.0	60.0	
2	2.4	59,310.0	0.2	Elastic Element					

*Note: Backfill element locations and properties remained unchanged.

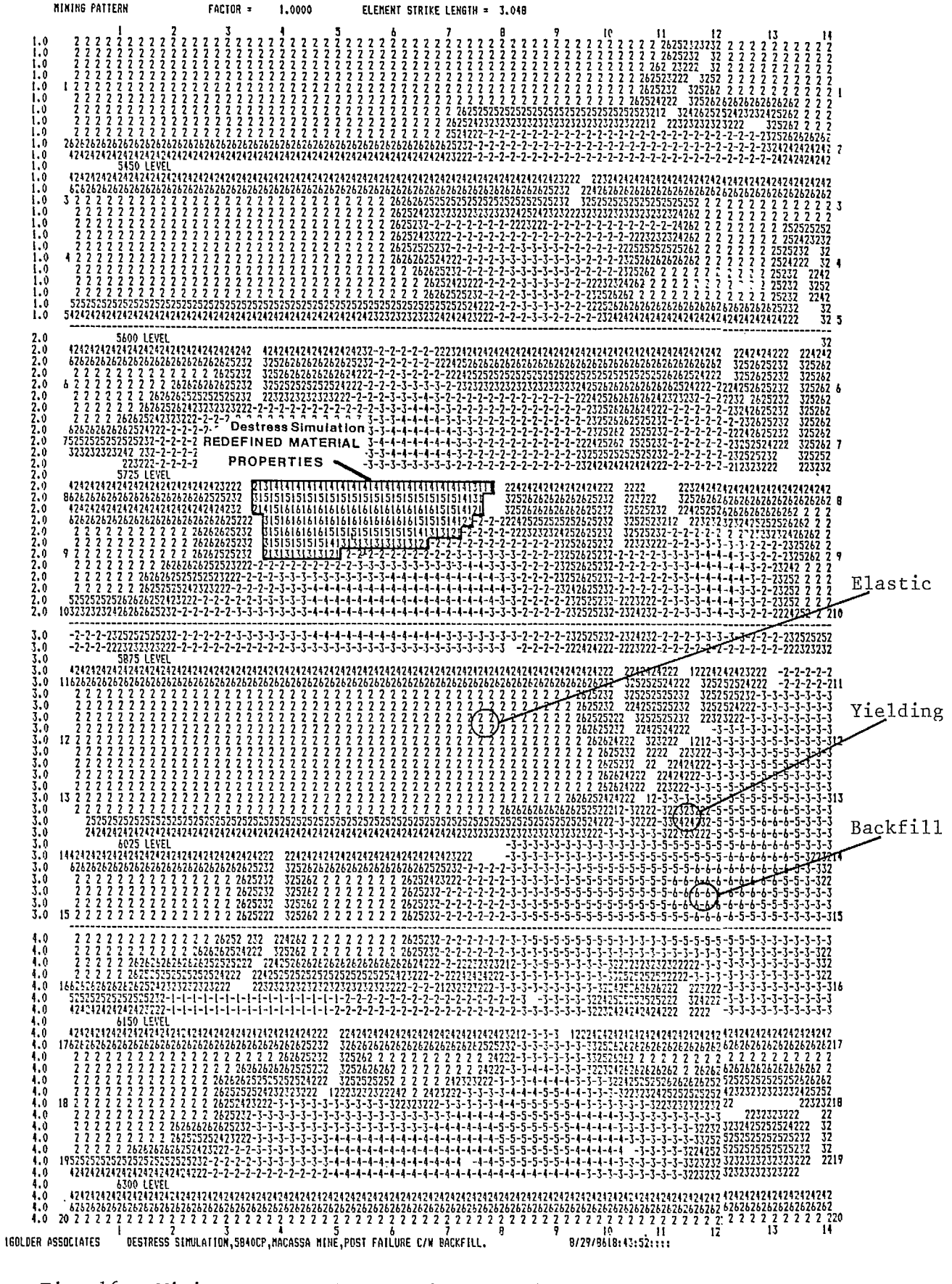

Fig. 16 - Mining pattern layout with redefined material properties for the 58-40 crown pillar only - destress simulation.

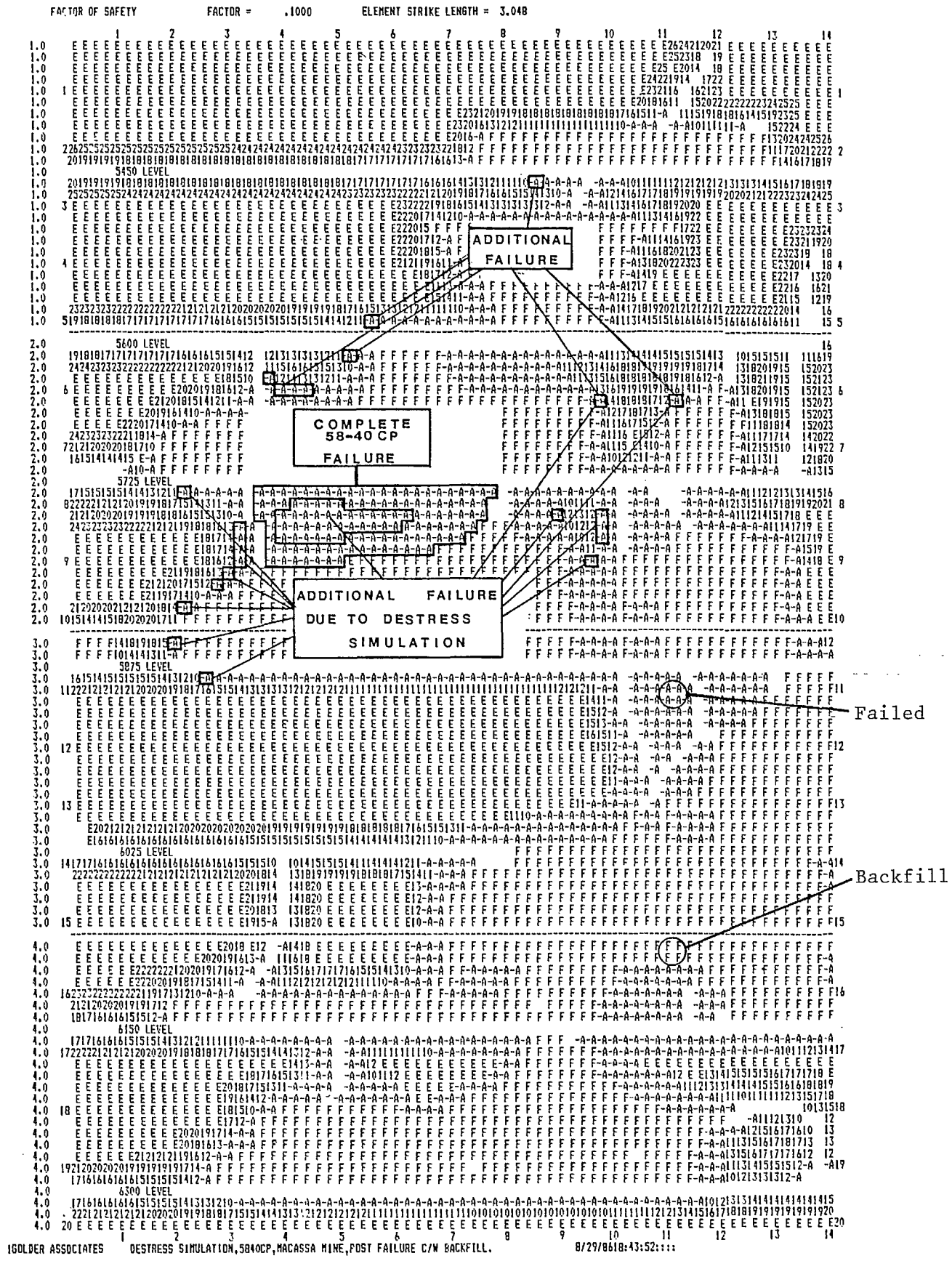

Fig. 17 - Strength/stress ratios displaying limited effect of destress simulation on surrounding pillars - destress simulation.

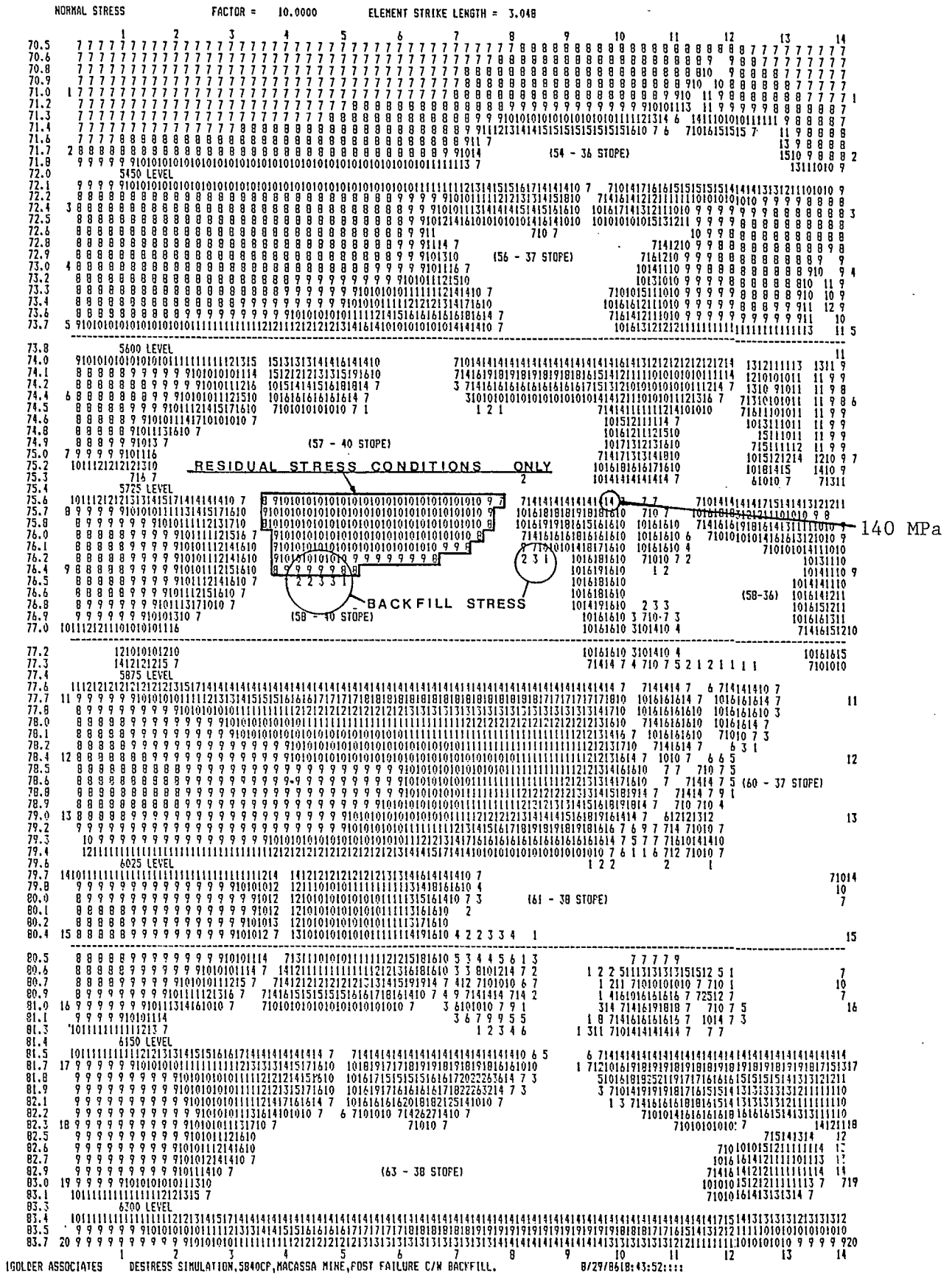

Fig. 18 - Perpendicular stresses with residual stress conditions of the 58-40 crown pillar highlighted - destress simulation.

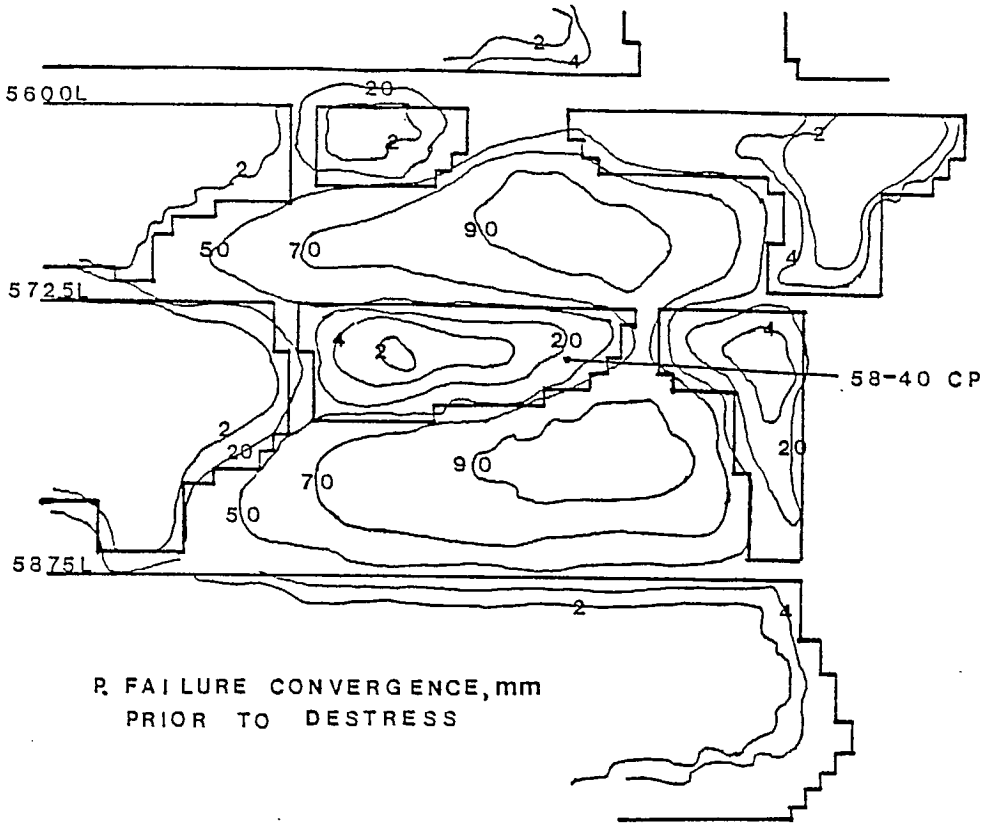

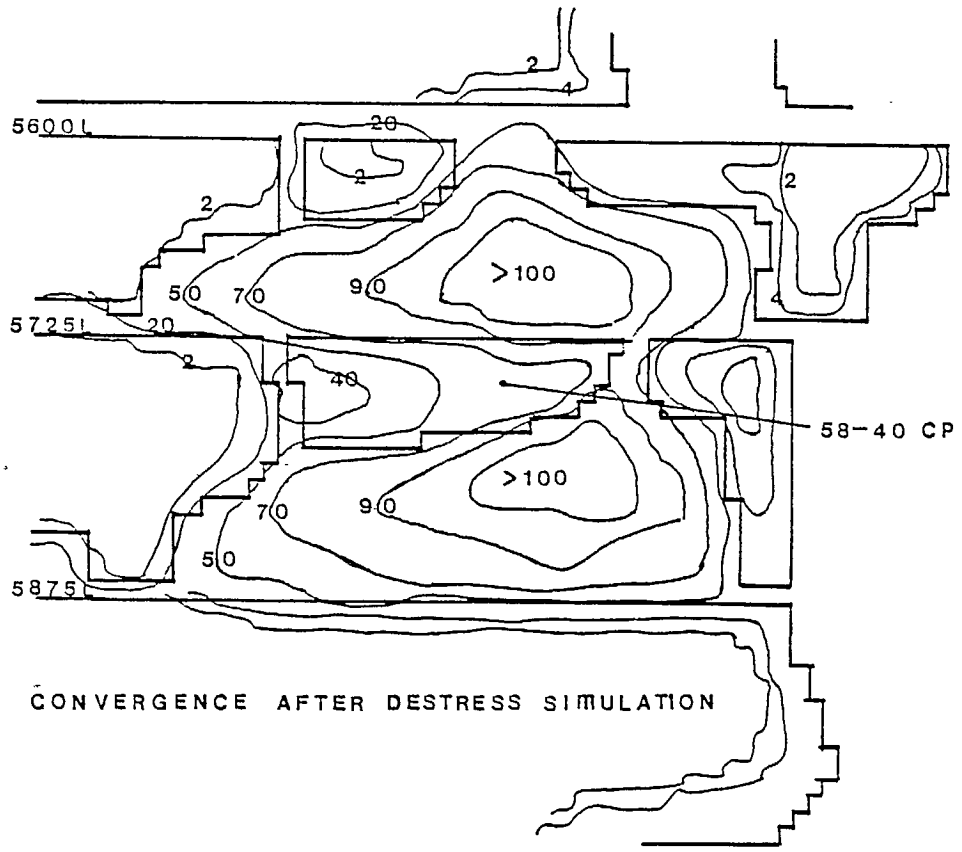

Fig. 19 - Convergence contours before and after the destress simulation.

At the same coordinates as the tape extensometer pins were located in the 58-40 stope (just below the 58-40 crown pillar) and on the 5725 level (Figures 20 and 21), the predicted differential convergences were obtained by subtracting the convergence values before and after the destress simulation at specific element locations. Figure 22 shows the measured differential convergences versus the predicted values from the NFOLD model.

A good proportion of the convergence measured with pins 58.5 to 58.2 was predicted by the NFOLD analyses. However, pin 58.1 measured only a fraction of the convergence that the NFOLD models expected. It was known that Hole No. 1 of the destress layout had not been loaded and possibly a small intact core was still present. The difference in the convergence results suggested this to be the case.

It should be noted that as of July 30, 1986, very poor agreement between the actual convergences measured and predicted by NFOLD occurred for those pins located on the 5725 level.

Since this period more recent measurements have indicated additional convergence at the 58-40 stope pin locations and substantially more convergence at those pin locations directly above the 58-40 crown pillar. The recent data suggests that possibly the destress holes might have been located nearer to the 5725 sill horizon and that this same area may still have some burst potential (it was assumed earlier to be highly fractured and therefore not destressed during the blast).

The NFOLD computer mining simulations were considered a success as they had accurately indicated the failure areas prior to the destress blast, determined that destressing the pillar had a limited effect on the surrounding openings, and predicted convergence values that agreed reasonably well with the underground measurements, particularly for the 58-40 stope convergence stations.

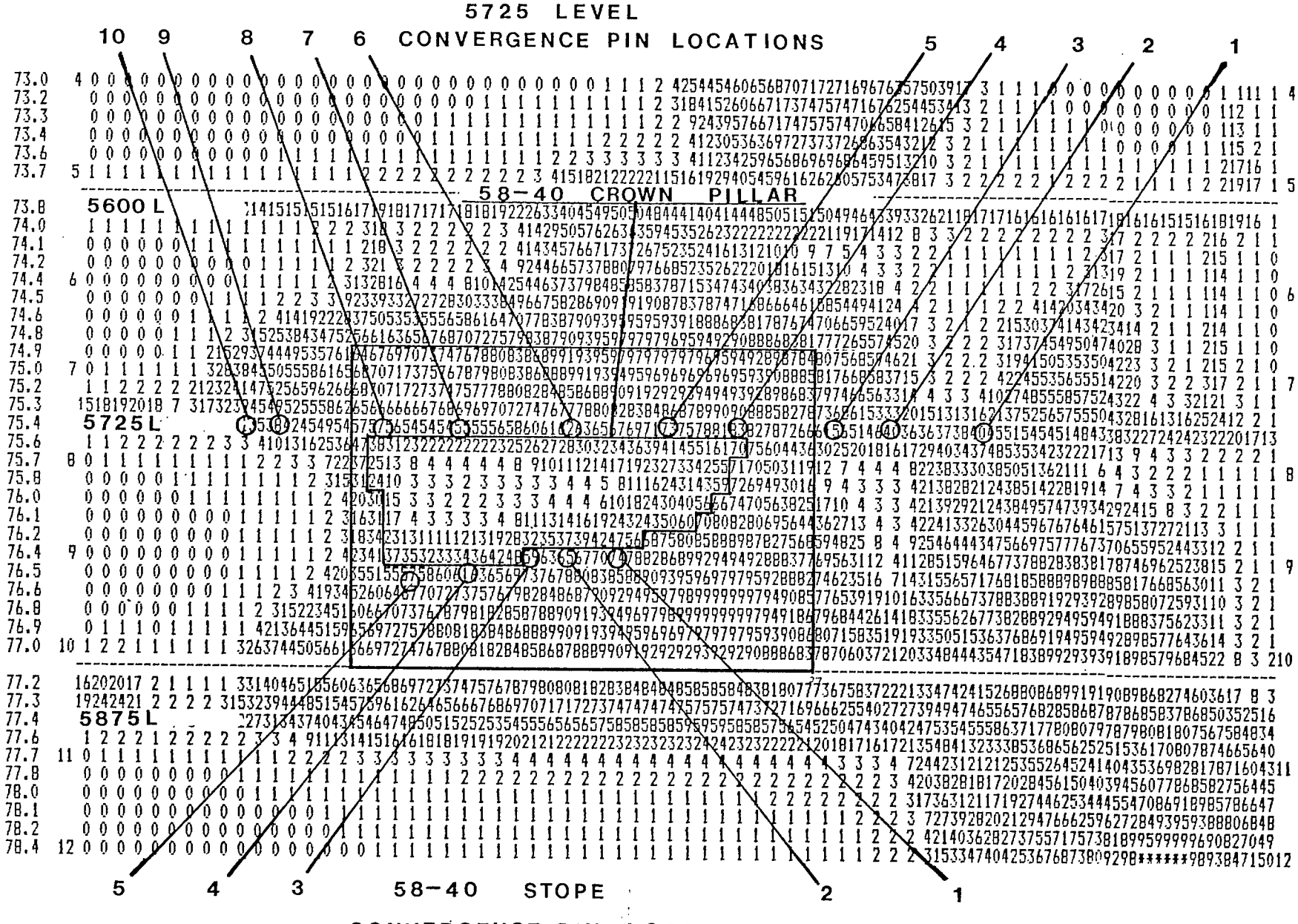

Fig. 20 - Non-linear NFOLD model convergence prior to destressing.

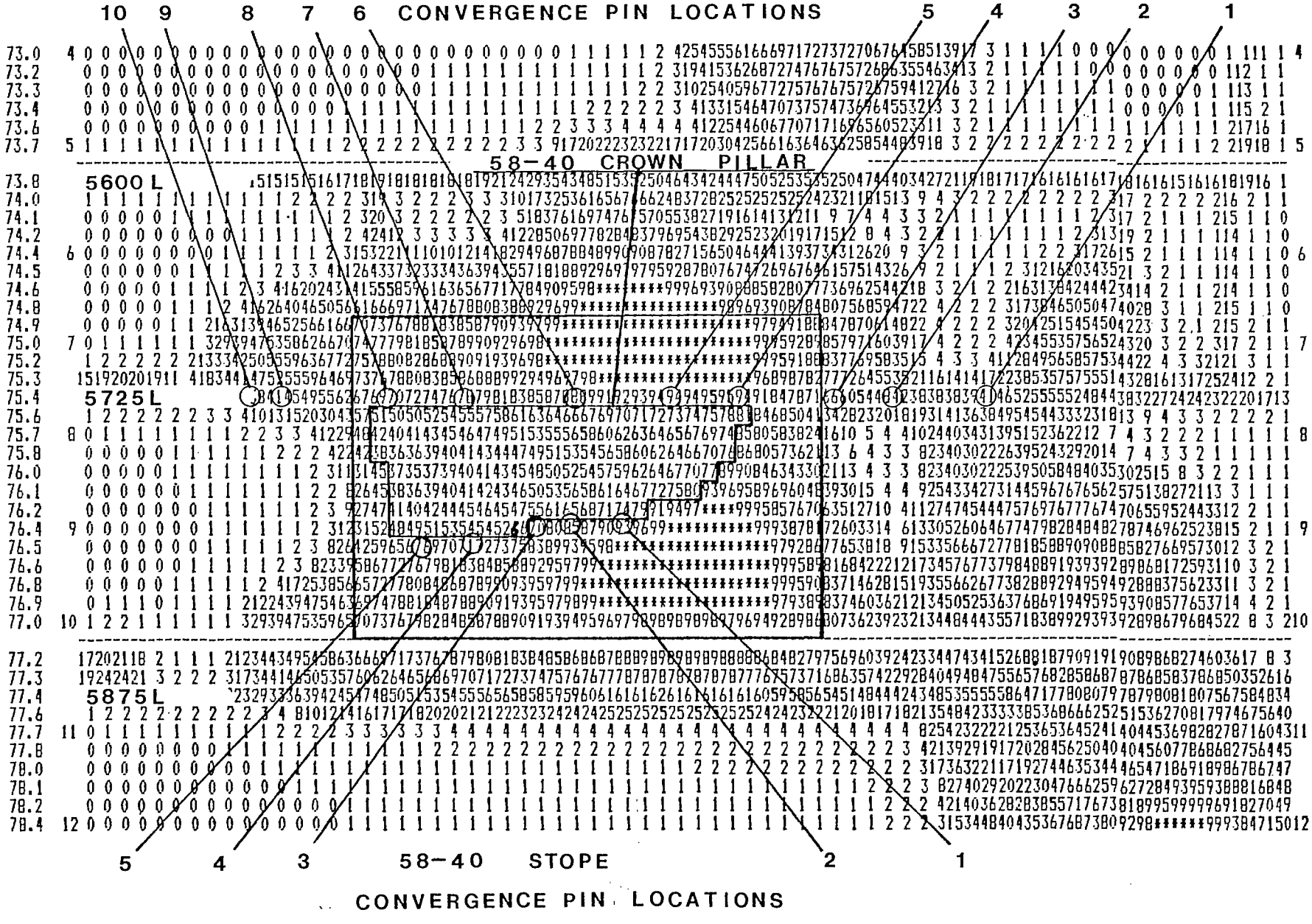

Fig. 21 - Convergence after non-linear NFOLD destress simulation.

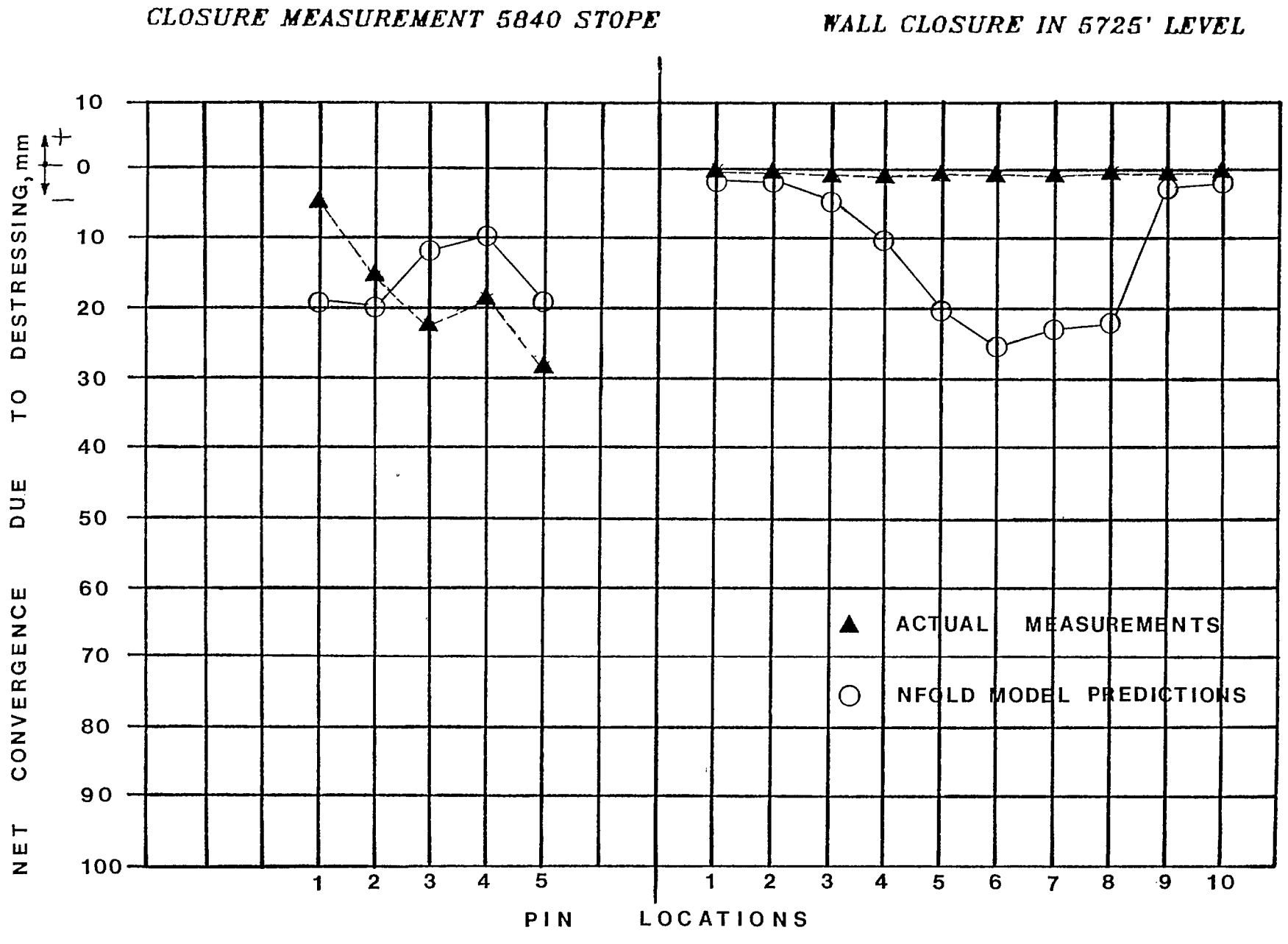

Fig. 22 - Comparisons between the NFOLD predicted convergence versus actual measurements as of July 30/86.

DISCUSSION OF RESULTS

CORRELATION OF COMPUTER SIMULATION, CONVERGENCE AND MICROSEISMIC ACTIVITY

1) Tape convergence measurements indicated the destress blast resulted in the maximum convergence occurring in the western part of the upper 58-40 stope suggesting adequate fracturing of the 58-40 pillar in this vicinity. Much less convergence was measured on the eastern side of this crown pillar.

   Microseismic activity also indicated a clustering of seismic events more heavily populated on the western side of the 58-40 pillar with only a few events on the eastern one-third. Most of the events were contained within, or very near to the ore seam, suggesting an immediate fracturing and local disturbance.

   Destress simulation using the NFOLD model did not suggest as large a discrepancy in differential convergence as was suggested by the underground measurements. The assumption was that if the destress was successful, all elements within the crown pillar would have failed.

   The three methods together verified that considerable fracturing of the western portion of the 58-40 crown pillar occurred, but raised the suspicion as to whether or not the eastern portion of the pillar as well as that immediately below the 5725 level had been adequately destressed.

2) Very little differential convergence was measured from pin installations on the 5725 level directly above the 58-40 crown pillar as a result of the destress blast.

   The top portion of the 5840 crown pillar was generally void of microseismic activity as a result of the destress blast. This was true for all source location algorithms evaluated.

   The NFOLD computer mining simulation model indicated that the top portion of the 58-40 crown pillar was in a failed state prior to the

destress blast. Examination of diamond drill cores also indicated a fractured zone engulfing an intact central pillar core. Differential convergence predicted by the model destress simulation was somewhat more pronounced that that actually measured on the 5725 level, possibly indicating a greater zone thickness having failed than simulated by the NFOLD model prior to destressing.

The other possibility is that of the assumed upper fractured zone being actually intact and unfractured with high stress loading. The destress blast by design did not fracture this zone, but the presence of a reduced actual powder factor relative to that designed could also have been responsible for a reduction in blast fracturing and induced yielding. Recent measurements from the convergence stations now seem to support this concept.

3) Most of the microseismic activity following the destress blast was contained within the 58-40 crown pillar with isolated events occurring in the east and west 58-40 stope abutments, and for some source location algorithms there was some scatter down to the 57-40 stope and buttressing pillar below the 5875 level.

Destress simulation using the NFOLD model resulted in increased failure mainly within the 58-40 crown pillar with only a few additional elements failing within the 36-waste pillar, western 58-40 stope outline, and eastern 57-40 crown pillar buttress.

Convergence measurements were not available over this large an area.

The computer modelling and microseismic results show that sufficient buttressing pillars were present and the level of extraction low enough that the disturbance of the destress blast was restricted to the immediate area of the 58-40 crown pillar. For the mine geometry that was present the effects of the blast were minimal.

MINING TO DATE

Further verification of the success of the 58-40 crown pillar destress would involve the return to actual mining within the pillar with minimal difficulty.

Two separate longwall blasts, the first on July 30, 1986, and the second on September 20, 1986, had widely varying effects.

When the July 30, 1986 longwall blast occurred, the Electro-Lab MP-250 microseismic system was still operational. Source locations following the first production blast (after 02:45 a.m.) using the USBM 'Least Squares', Block and Simplex methods were determined in order to evaluate the effectiveness of the former destress blast. Some clustering of events, Appendix B, occurred near the longwall blast location, but in general the 58-40 crown pillar was void of events.

More event location scatter occurred for this production blast compared to the destress blast. Transverse and longitudinal mine plans demonstrated a large number of off-seam locations suggesting an alignment along a cross-cutting structure to the ore seam. Two such structures could be identified (section 43+00 and section 39+00) with reasonable confidence as all source location methods produced the same pattern.

One hundred and forty events were examined (Figure 23) with the event size categories by percent frequency population as follows:

Event Classification	% Frequency
Small	18.6
Intermediate	70.0
Large	11.4
Gould (WFR)	N/A

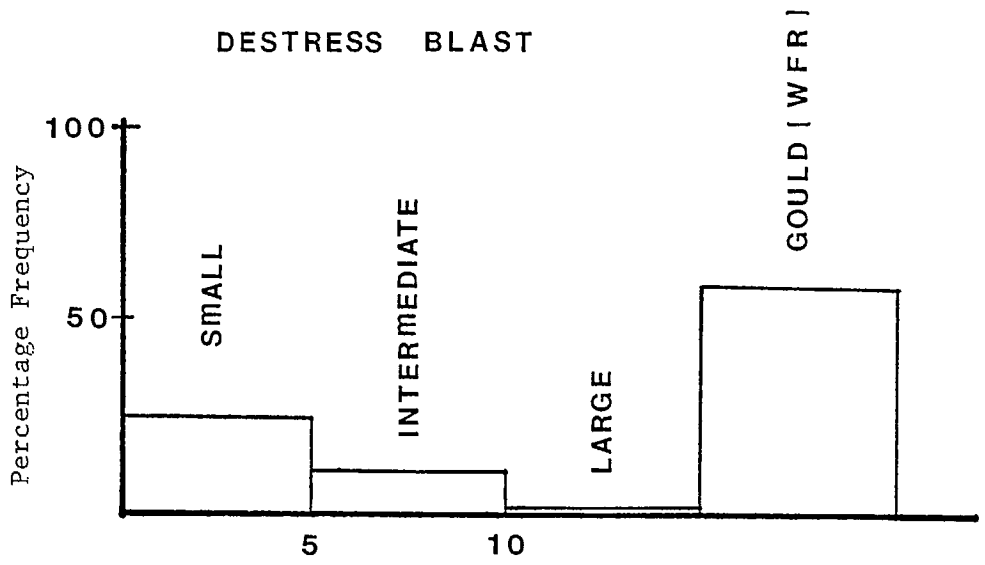

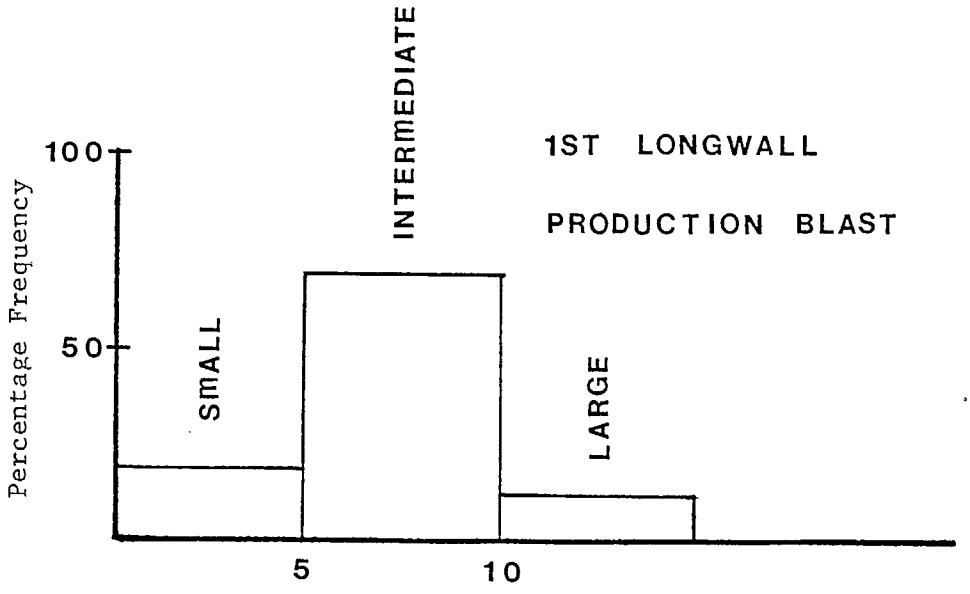

Fig. 23 - Percent frequency microseismic event dispersion.

The microseismic results indicated that:

1) Most of the 58-40 crown pillar had been successfully destressed;
2) There was a much greater scatter of event source locations than for the destress blast;
3) Cross-cutting features were suggested (faults, dykes) as some alignment to the events was observed.

The second longwall blast consisted of nineteen 2.4 m long blastholes (horizontal) initiated near the earlier No. 1 destress blast hole that was not loaded. Shortly after, a low energy burst resulted in a considerable deformation of stulls and rock boltheads in the stope. Differential convergence of 33 mm occurred at convergence pin 58.1 where earlier (destress blast) minimal convergence had been measured. The earlier suspicions had been confirmed, but now the feeling that the pillar was fully destressed seemed a more likely possibility. No microseismic event locations were obtainable as the system had been removed.

As a safety measure for the remaining longwall mining, it was decided that three 7.6 m long destress holes would be drilled regularly in advance of the longwall face. This destressing measure would be continued if further convergence occurred as mining of the longwall progressed westwards. Little differential convergence would suggest adequate destressing and convergence had already taken place, and these additional destress holes would be discontinued.

FUTURE MINING CONSIDERATIONS

Destress blasting was reasonably successful on the 58-40 crown pillar, but assessing the correct moment to destress is not always a simple matter.

The three different methods used in analyzing the effectiveness of the destress blast, underground convergence measurements, microseismic source location, and computer mining simulation, proved that none of the individual

methods were foolproof. Together, however, they provide an excellent set of tools for the mining staff to fully comprehend the ground conditions under burst potential situations. Visual observation by the critical eye provides a further means of verification whether results from the three methods seemed to represent actual conditions.

Of the three methods, only the computer mining simulation model, if adequately calibrated, can provide clues regarding future mining layouts, future burst potential pillars, and whether a future destress blast will create a safer environment or initialize a rapid succession of rockbursts over a large mining area.

In some mines where the ore extraction ratio is much higher than in the vicinity of No. 3 shaft at Macassa, factors of safety (pillar strength/pillar stress) may be only slightly greater than 1.0 for several crown pillars. This means that the good intentions of a destress blast, even though well designed, could still result in an incremental stress transfer to these extremely meta-stable areas. The generation of multiple rockbursts within a short time period would be likely.

It is important to examine various mining scenarios through modelling and choose the best extraction sequencing. This is not an easy task, but a necessary one to devote considerable time to, as once a method of attack is decided on it is very difficult to implement another.

CONCLUSIONS

1) The Macassa Mine generally experiences its larger rockbursts associated with the mining of crown pillars. Three documented rockbursts along with considerable ground deterioration suggested that the 58-40 crown pillar required destressing.
2) Bursting potential arises, not only because of high stress conditions

within a crown pillar, but is also very dependent on the ore seam material stiffness being greater than the hanging wall/footwall mine stiffness.

3) It is advisable that adequate instrumentation is in place prior to an area experiencing rockbursts. This instrumentation should consist of both convergence and stress measuring devices for local monitoring, and a microseismic data acquisition system for mine-wide monitoring. The presence of instrumentation results in easier calibration of computer mining simulation models so that 'predicted' equals 'observed'.

4) The actual blast implemented compared to the actual blast design conceived resulted in a much lower powder factor, and yet a fairly successful destressing took place as witnessed by the convergence results and microseismic source location plots.

Further analysis using the NFOLD computer model revealed that the actual intact core of the 58-40 crown pillar was smaller than at first thought in the western section, and a mismatch in differential convergence (after destressing) predicted in the eastern section by the model versus actual convergence measured, suggested that it was not successfully destressed there.

Where lower stressed crown pillars are to be conditioned the suggestion is that a much higher powder factor would be used to generate full pillar failure.

5) The three engineering tools, tape convergence measurements, microseismic event locations, and computer mining simulation were all necessary to get a full understanding of the success of the destress blast, and together they provided the following:

- bursting was essentially confined to the 58-40 crown pillar after destressing;
- some areas (eastern section) of the 58-40 crown pillar did not fail and

would require further destressing;

- little additional convergence or seismic activity occurred after destressing if an area was designated as already having failed prior to the blast.

6) Future burst potential geometries can be evaluated using the NFOLD model before the actual mine extraction occurs, and future destress simulations attempted to determine the correct timing of a destress blast. If multiple crown pillar bursting is suggested as a result of the simulation then multiple destress blasts might be necessary to transfer stress away from the crown pillars to the abutments. Simultaneous destress blasting would be a desirable feature in this case.

7) The mining method used in destressed ground must be flexible to allow the drilling and initiation of further destress holes if required in advance of the face. The longwall method incorporates this procedure so that the working environment is less hazardous.

ACKNOWLEDGEMENTS

The authors would like to thank the management of both Lac Minerals and CANMET for their permission to present this paper through the Canada/Ontario/ Industry Rockburst Project. Special thanks to A. Makuch who ran the initial DZTAB model and provided guidance during the installation of the Electro-Lab MP-250 microseismic system. Additional thanks go to D.G.F. Hedley, P. Rochon, and B. Arjang, Research Scientists at Elliot Lake Laboratory, and P. MacDonald, INCO Ltd., for their assistance, and to Golder Associates, Toronto during the initial NFOLD model discussions and accessibility to the model itself.

REFERENCES

1. Arjang, B. and Vaillancourt, G., "Field stress determinations at Macassa Mine, Kirkland Lake, Ontario"; Division Report MRP/MRL 85-63(TR); CANMET, Energy, Mines and Resources Canada; 1985.

2. Arjang, B. and Nemcsok, G., "Review of rockburst incidents at the Macassa Mine, Kirkland Lake"; Division Report M&ET/MRL 87- (TR); CANMET, Energy, Mines and Resources Canada; 1986.

3. Blake, W., "Destressing to control rock bursting"; in Underground Mining Methods Handbook, Chapter 7; W.A. Hustrulid (Ed.); Society of Mining Engineers, AIME, New York, New York; 1982.

4. Cook, J.F. and Bruce, D., "Rockbursts at Macassa Mine and the Kirkland Lake mining area"; Proc. Symp. Rockbursts Prediction and Control; IMM, London, United Kingdom; 1983.

5. Nemcsok, G., "General mine geology description"; Visitor's Handout Guide, Macassa Mine.

6. Quesnel, W.J. and Hong, R., "The use of rock mass conditioning (destressing) for the safe recovery of a rockburst prone crown pillar, Macassa Division, Lac Minerals Ltd"; Ground Control Symp., Haileybury School of Mines; 1986.

7. Salamon, M.D.G., "Energy considerations in rock mechanics: fundamental results"; J. S. African Inst. Min. & Met., vol. 84, No. 8, pp 233-246, August 1984.

APPENDIX A

MICROSEISMIC SOURCE LOCATION PLOTS

AS A RESULT OF THE DESTRESS BLAST

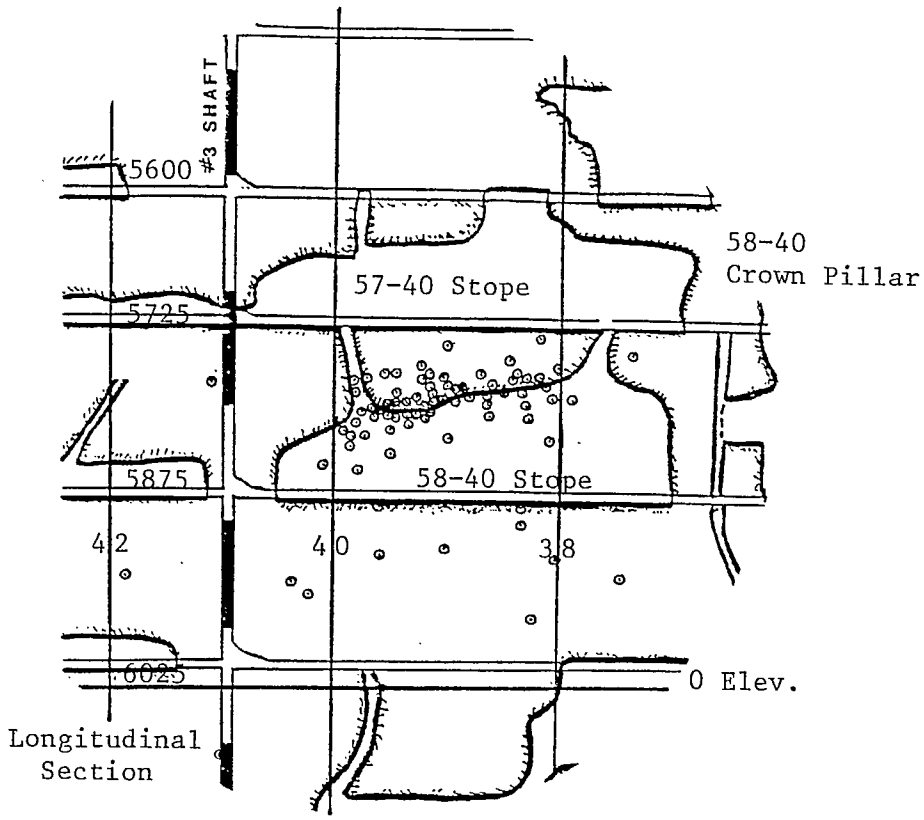

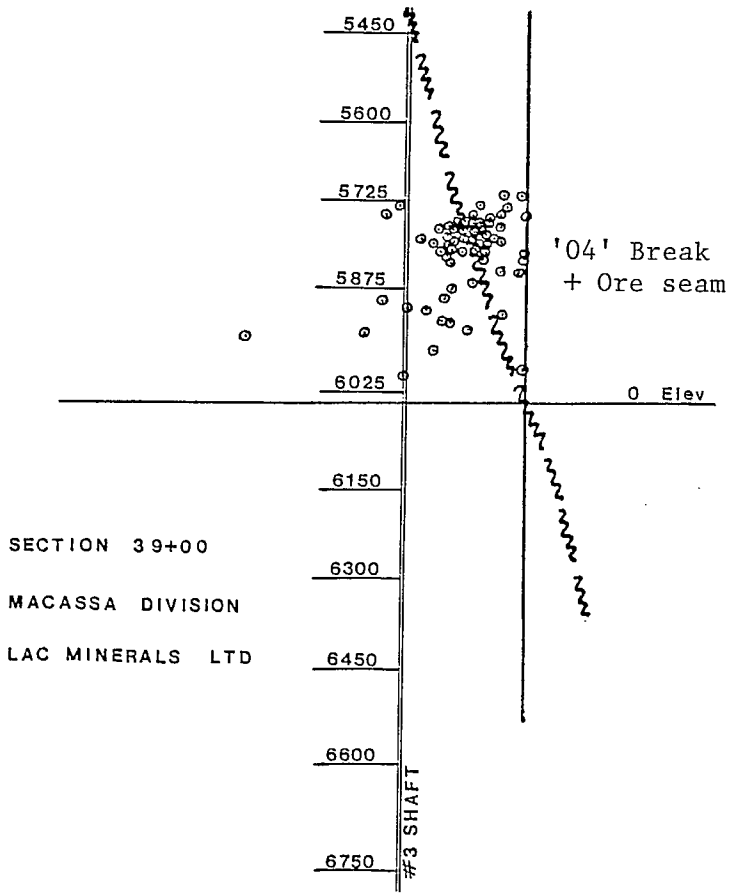

A-1 - USBM microseismic events activated - destress blast.

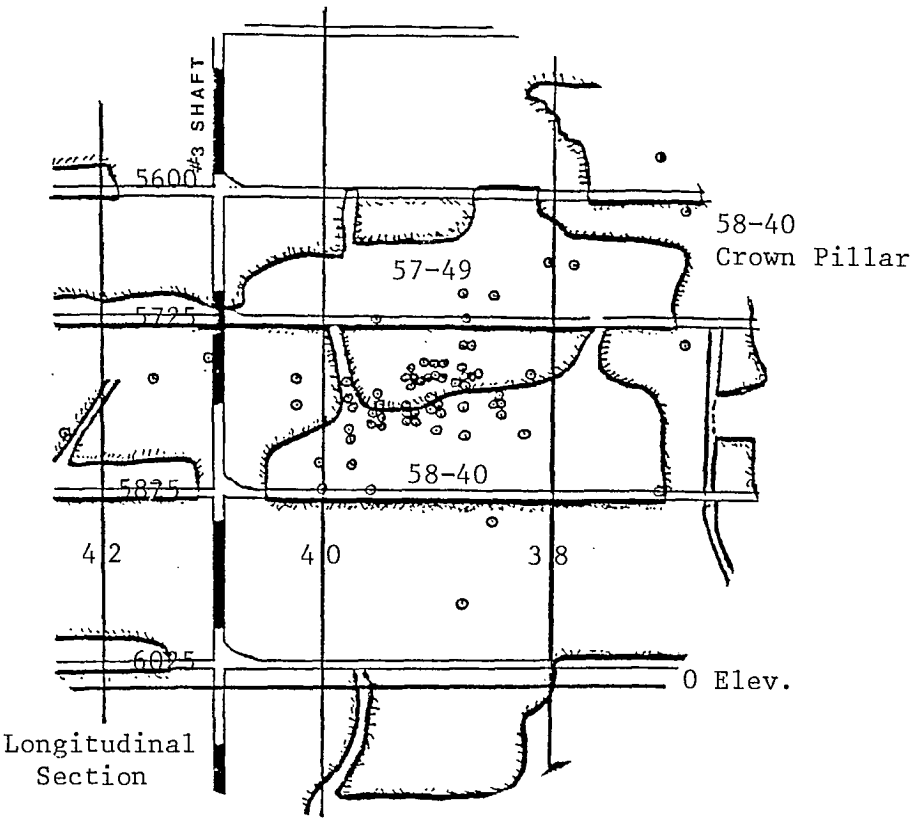

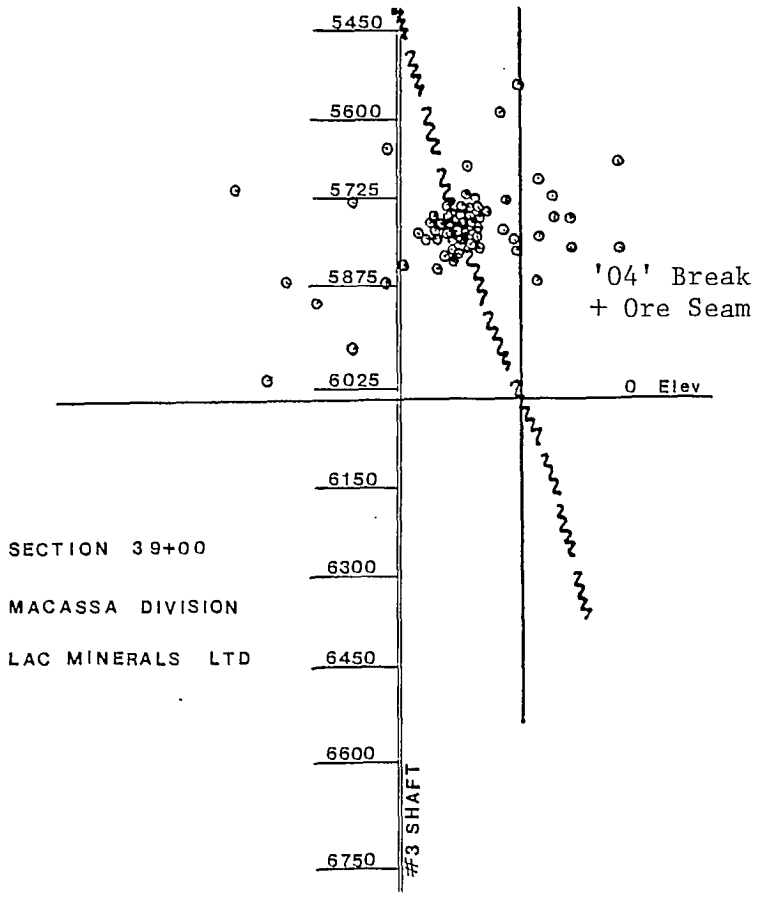

A-2 - Block microseismic events activated - destress blast.

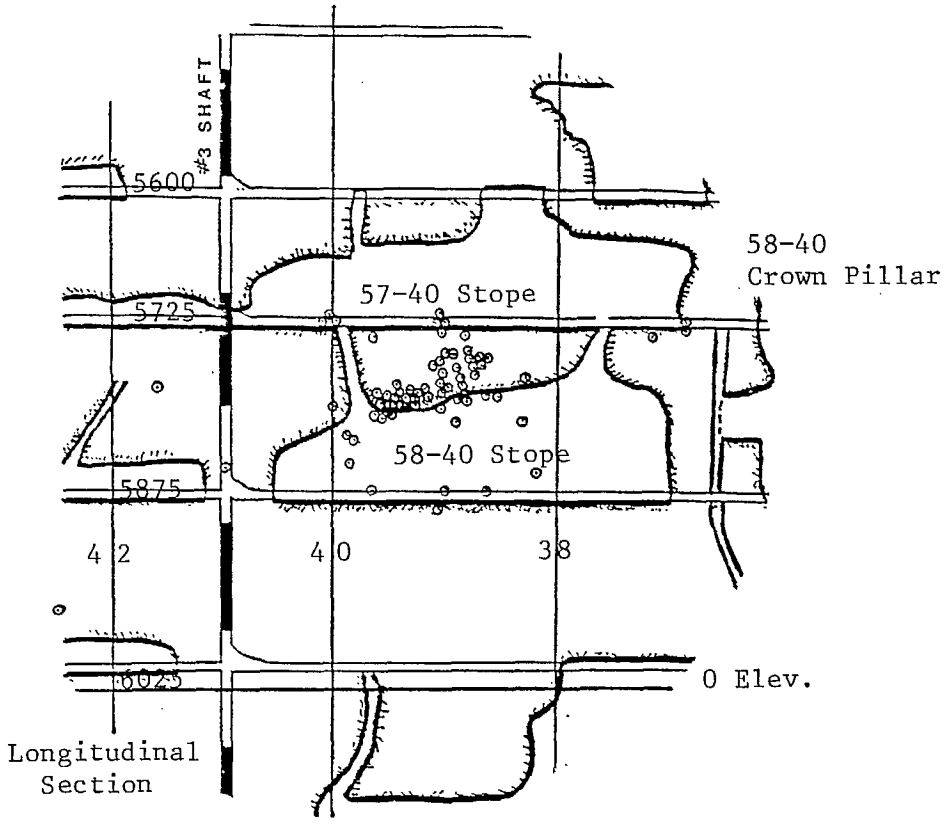

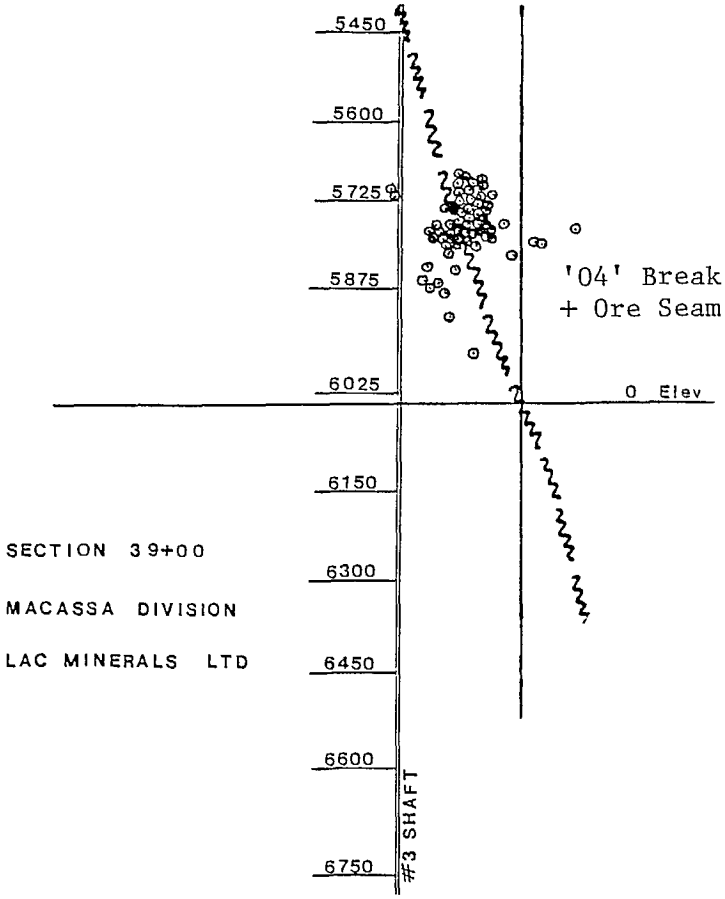

A-3 - Simplex microseismic events activated - destress blast.

APPENDIX B

MICROSEISMIC SOURCE LOCATION PLOTS

FIRST PRODUCTION BLAST 58-40 CROWN PILLAR

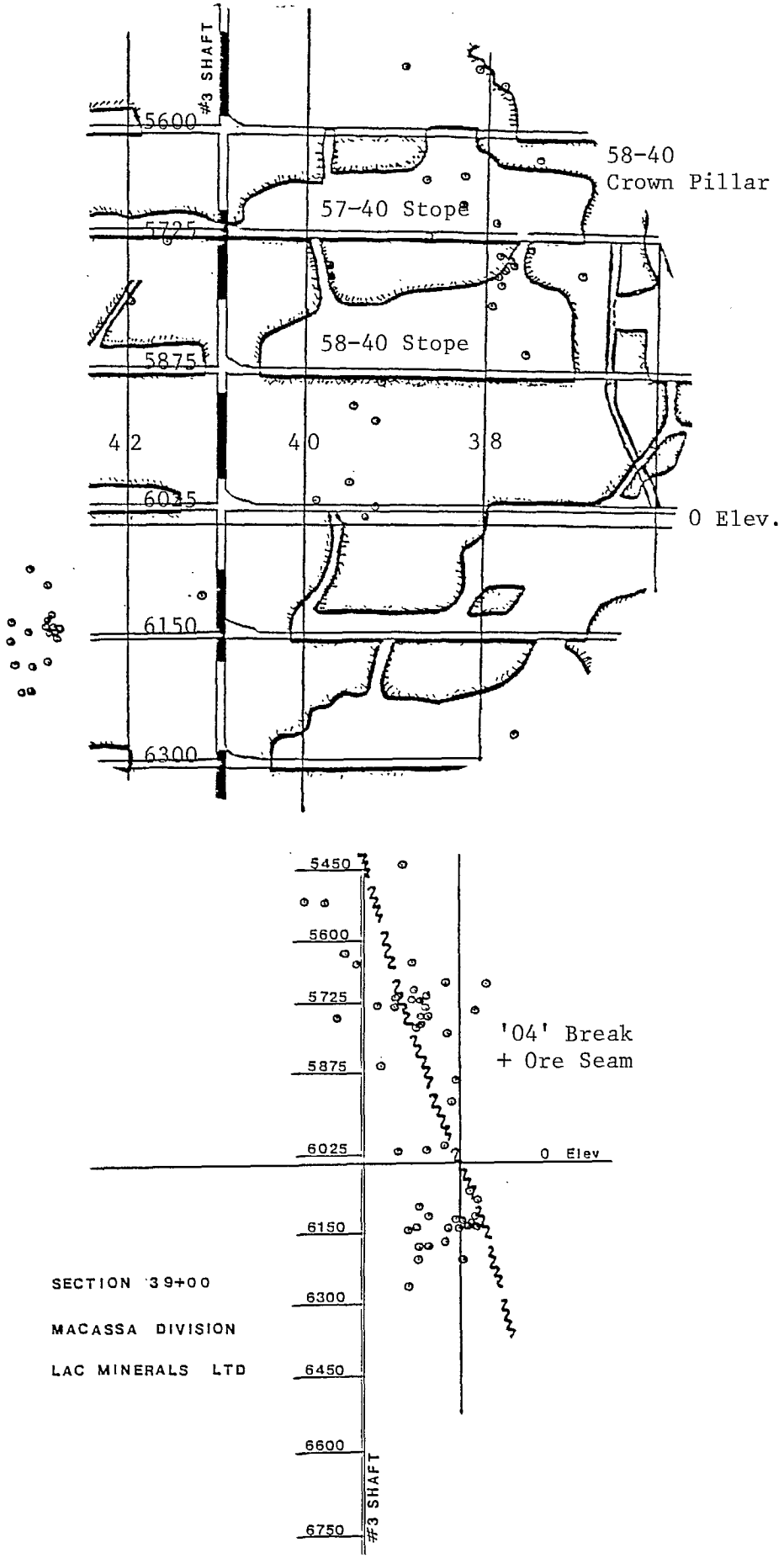

B-1 - USBM Microseismic events activated - production blast.

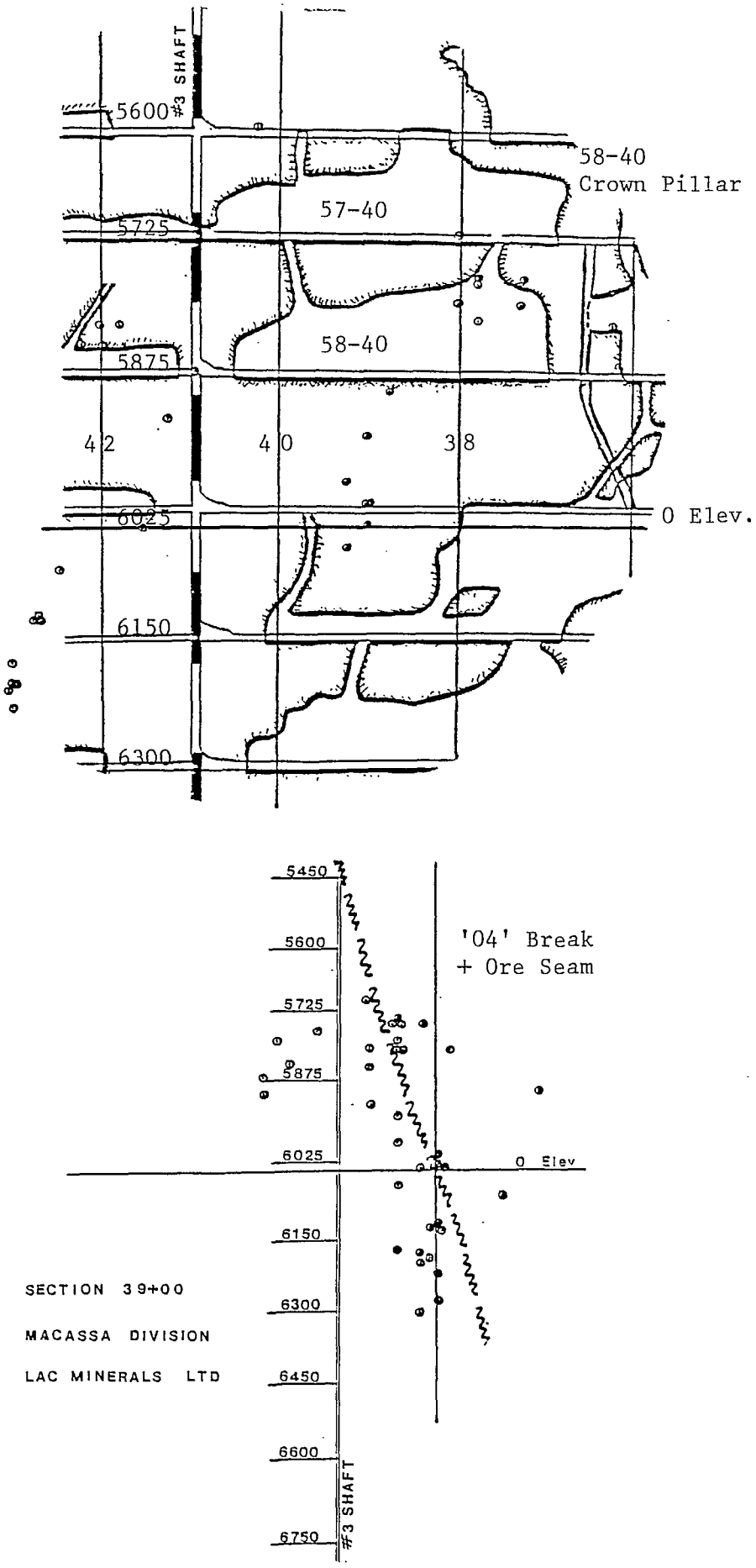

B-2 - Block microseismic events activated - production blast.

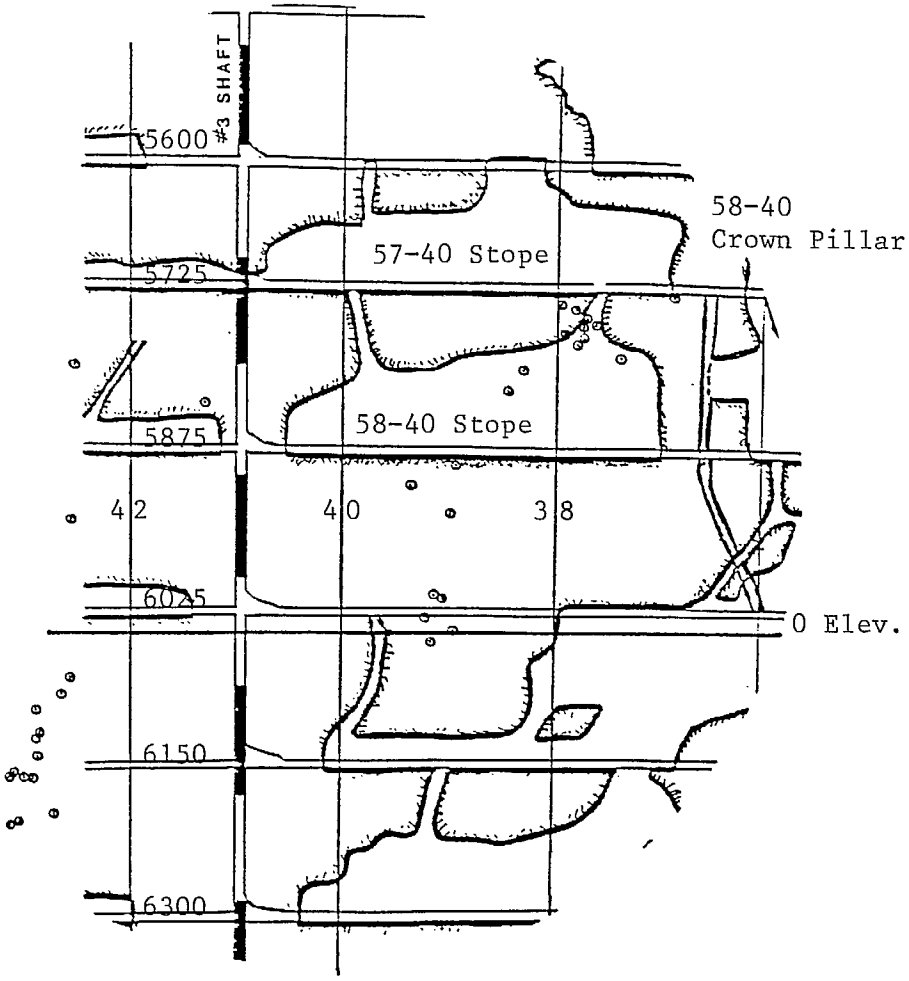

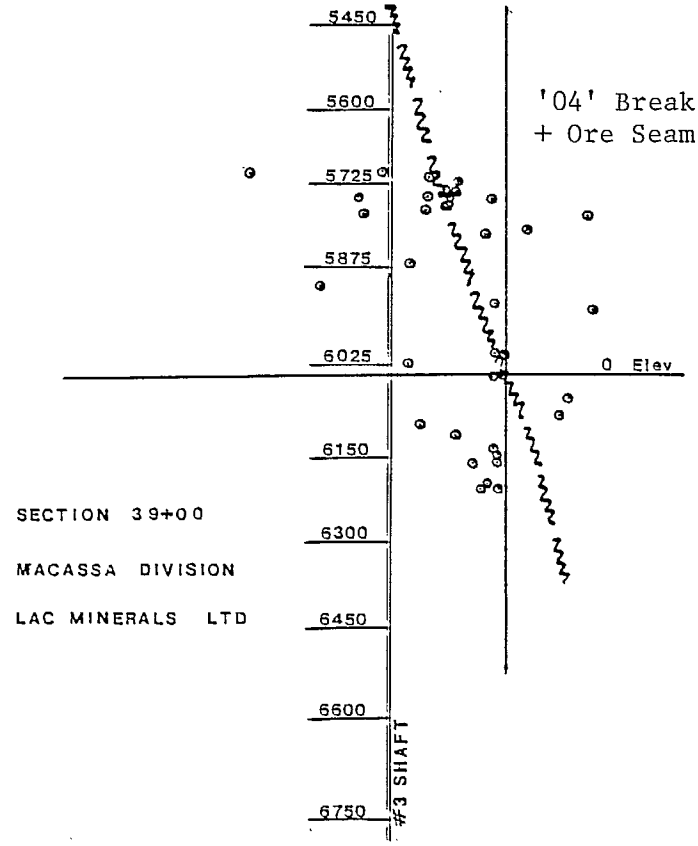

B-3 - Simplex microseismic events activated - production blast.